The 2nd Asian Workshop on Molecular Spectroscopy

Date : March 9-10, 2018
Venue : Department of Physics, National Central University

Sponsor

Committees

International Committee:

J. T. Hougen, National Institute of Science and Technology, U. S. A.

A. J. Merer, Institute of Atomic and Molecular Sciences, Academia Sinica, Taiwan, and U. of British Columbia, Canada

Y.- P. Lee, National Chiao Tung U., Taiwan

T. Amano, Jet Propulsion Laboratory, California Institute of Technology, U. S. A.

M. Baba, Kyoto U., Japan,

S.-M. Hu, University of Science and Technology, China

C. H. Kwon, Kangwon National U., Korea

L.-H. Xu, U. of New Brunswick, Canada

Local Organizing Committee:

Y.-C. Hsu, National Central U., Taiwan, and Institute of Atomic and Molecular Sciences, Academia Sinica, Taiwan

K. Takahashi, Institute of Atomic and Molecular Sciences, Academia Sinica, Taiwan,

B.-C. Chang, National Central U., Taiwan

W.-Y. Cheng, National Central U., Taiwan

Y.-J. Wu, National Synchrotron Radiation Research Center, Taiwan

Program

Time	March 9 (Day 1)
8:00~8:45	**Registration (Hakka College, NCU)**
8:45~9:00	**Opening Remarks** **Hsuan-Yi Chen(NCU), J. Hougen (NIST)**
	Ro-vibrational Spectroscopy Chair: Prof. K. Kobayashi (U. Toyama)
9:00~9:20 **A1**	**Combined analysis of the rotational Lines and the electronic transitions of CH^+: revisiting the Λ-doubling in $^1\Pi$ states** T. Amano (JPL)
9:20~9:40 **A2**	**Rotational spectra of water adducts of fluorinated pyridines: fluorination effects on the interaction topologies** Q. Gou (Chongqing U.)
9:40~10:00 **A3**	**Absorption spectroscopy of H_2O and CH_4 with amplitude- and phase-modulation** W.-L. Chen (NTHU)
10:00~10:20 **A4**	**Real-time ion imaging-based rotational/vibrational spectroscopy of nitrogen dimer** K. Mizuse (Tokyo Int. Tech.)
10:20~10:40	**Coffee break**
	Electronic Spectroscopy Chair: Wen-Bih Tzeng (IAMS)
10:40~11:00 **A5**	**New electronic states of YO in the UV region** A. S. C. Cheung (U. Hong Kong)
11:00~11:20 **A6**	**Low-lying electronic states of scandium monocarbide, ScC, observed by laser-induced fluorescence** A. Merer (IAMS and U. British Columbia)
11:20~11:40 **A7**	**Spectroscopy of the B(1)-X(0^+) transitions of PbO with 10-MHz precision and control of the translational motion with a microwave field** K. Enomoto (U. Toyama)
11:40~12:00 **A8**	**Substituent effect on electronic transition energy of multi methyl-substituted benzyl radicals** S. Lee (Pusan Nat. U.)

12:00~13:00	**Lunch (NCTS, NCU)**
	MW Spectroscopy Chair: Yasuki Endo (NCTU)
13:10~13:30 **A9**	**Microwave study of internal rotation in para-tolualdehyde: local versus global symmetry effects at the methyl-rotor site** J Hougen (NIST)
13:30~13:50 **A10**	**Hyperfine splittings of methanol in the first torsional state** L.-H. Xu (U. New Brunswick)
13:50~14:10 **A11**	**Microwave zeman effect of methanol** K. Kobayashi (U. Toyama)
14:10~14:30 **A12**	**Dimers of hydrofluoroalkanes by microwave spectroscopy** G. Feng (Chongqing U.)
14:30~15:10	**Coffee break** **Group photo**
	IR spectroscopy / Cluster / Theory Chair: Jer-Lai Kuo (IAMS)
15:10~15:30 **A13**	**Simulation of realistic vibrational spectra line-shapes: anharmonic effects on the band position and transition intensities** M. Biczysko (Shanghai University)
15:30~15:50 **A14**	**Theoretical study on the vibrational states for HO_3 system based on full-dimensional potential energy surface** X. Hu (Nanjing U.)
15:50~16:10 **A15**	**The vibrational levels of the Ã state of C_3Ar studied by hole-burning experiments and ab initio calculations** Y. J. Wang (IAMS)
16:10~16:30	**Coffee break**
	Dynamics Chair: Thomas Schultz (UNIST)
16:30~16:50 **A16**	**Halogen molecular elimination from halogen-containing compounds in atmosphere Using cavity ring-down spectroscopy** K. C. Lin (NTU)
16:50~17:10 **A17**	**Dependence of proton-transfer dynamics on the configuration of diols as effective Brønsted bases** Y.-J. Kim (UNIST)
17:10~17:30 **A18**	**Excited-state proton-transfer dynamics of 6-hydroxyquinoline with amphiprotic weak acid in a nonpolar liquid phase solvent**

	K. E. Mun (UNIST)
17:30~17:50 **A19**	**Study on nonradiative decay and photoisomerization route of cinnamic acid derivatives** T. Ebata (Hiroshima U.)
17:50~18:10 **A20**	**Laser-induced fluorescence study of CaH** **K. Watanebe (U. Toyama)**
18:20~20:20	**Buffet (625, Physics, NCU)**

Time	March 10 (Day 2)
8:30~9:00	**Registration (Hakka College, NCU)**
	PAHs spectroscopy Chair: Masashi Tsuge (Hokkaido U.)
9:00~9:20 **B1**	**Ultrahigh-resolution spectroscopy of polycyclic aromatic hydrocarbons** M. Baba (Kyoto U.)
9:20~9:40 **B2**	**Comb-referenced spectroscopy of polycyclic hydrocarbons** M. Misono (Fukuoka U.)
9:40~10:00 **B3**	**Infrared spectra of protonated and hydrogenated corannulene ($C_{20}H_{10}$) using matrix isolation in solid para-hydrogen** P. Sundararajan (NCTU)
10:00~10:20 **B4**	**Supersonic-jet laser spectroscopy of nonplanar aromatic hydrocarbon** A. Kanaoka (Kyoto U.)
10:20~10:40	**Coffee break**
	Free radicals Chair: Yu-Jong Wu (NSRRC)
10:40~11:00 **B5**	**Infrared spectrum of proton-bound nitrogen dimer N_2–H^+–N_2 in solid para-H_2** M. Tsuge (Hokkaido U.)
11:00~11:20 **B6**	**Analysis of infrared absorption spectra of solid methanol at low temperature after hydrogen atom bombardment** Y. Yarnall (George Mason U.)
11:20~11:40 **B7**	**Hydrogen abstraction from methyl formate by H-atom. Infrared absorption spectra of •$COOCH_3$ radical isolated in solid para-hydrogen.** K. Haupa (NCTU)
11:40~12:00 **B8**	**2C-R4WM Spectroscopy of the NO_3 $\tilde{B}\ {}^2E'$ - $\tilde{X}\ {}^2A_2'$** M. Fukushima (Hiroshima City U.)
12:00~13:00	**Lunch**
	Criegee Chair: Kaito Takahashi (IAMS)
13:10~13:30 **B9**	**Rotational investigation on the conformational preferences and reactivity of Criegee intermediates** Y. Endo (NCTU)

13:30~13:50 **B10**	**High resolution spectroscopy and reaction kinetics of simplest Criegee intermediates studied by mid-IR laser spectrometer** Y.-P. Chang (NSYSU)
13:50~14:10 **B11**	**High-resolution spectra of the simplest Criegee intermediate CH_2OO between 880 and 932 cm^{-1}** P.-L. Luo (NCTU)
14:10~14:30 **B12**	**Reaction of the Criegee Intermediate CH_2OO with HCl Investigated with a Step-scan Fourier-transform spectrometer** W. C. Liang (NCTU)
14:30~14:50 **B13**	**Theoretical calculation of UV spectrum for Criegee intermediates** C. Yin (IAMS)
14:50~15:10	**Coffee break**
	New spectroscopy technique Chair: Hiroyuki Sasada (Keio U.)
15:10~15:30 **B14**	**Photothermal interferometric gas sensing in hollow-core optical fibers** W. Ren (Chinese U. Hong Kong)
15:30~15:50 **B15**	**Direct frequency comb spectroscopy and its application** T. -W. Liu (NCU)
15:50~16:10 **B16**	**Narrow-bandwidth coherent-population-trapping resonance under polarization modulation** B. -W. Chen (NCU)
16:10~16:30 **B17**	**Effect of chloride ion in photoreaction of 4-aminobenzoic acid on silver surface investigated by the SERS spectroscopy and the DFT calculation** D. G. Yoon (Kangwon Nat. U.)
16:30~16:50	**Coffee break**
	Precision measurement Chair: Wang-Yau Cheng (NCU)
16:50~17:10 **B18**	**Relative intensity of a crossover resonance to Lamb dips** S. Okuda (Keio U.)
17:10~17:30 **B19**	**The Influence of atmospheric helium on secondary time standard** K.-H. Chen (NCU)
17:30~17:50 **B20**	**Dual-comb spectroscopy of acetylene $\nu_1+\nu_3$ vibration band** K. Iwakuni (JILA)

17:50~18:00	**Concluding remark** **Y.-C. Hsu (IAMS & NCU)**

A1

Combined Analysis of the Rotational Lines and the Electronic Transitions of CH^+: Revisiting the Λ-doubling in $^1\Pi$ States

S. Yu, B. J. Drouin, J. C. Pearson, and T. Amano
Jet Propulsion Laboratory, California Institute of Technology, Pasadena,
CA 91109, USA
e-mail: tamano@jpl.nasa.gov

THz rotational lines of CH^+ and its isotopologues have been observed in the range of 0.9-2.6 THz with JPL (Jet Propulsion Laboratory) frequency multiplication chains. They were analyzed together with the known $A^1\Pi - X^1\Sigma+$ band system data by using the Dunham formulation and the conventional vibration-rotation energy formula. The Λ-doubling splitting in $^1\Pi$ electronic states has been expressed as $\pm(1/2)qJ(J + 1)$ in most investigations. A Dunham analysis of the $A^1\Pi - X^1\Sigma^+$ band was carried out by Müller, and he used the same expression for the Λ-doubling.

However, it should be noted that the e-levels of $^1\Pi$ state interact with $^1\Sigma^+$ states, while the f-levels with $^1\Sigma^-$ states. For CH^+, the e-levels of $A^1\Pi$ are pushed upward largely from the interaction with the ground $X^1\Sigma^+$ state. The $^1\Sigma^-$ states are not known experimentally and they, if any, should lie high over the $A^1\Pi$ state. As a result the shifts of the f-parity levels are expected to be negligibly small. In general, there may be several $^1\Sigma$ states to interact with the $^1\Pi$ state, and the "Λ-doubling" energy term is given by

$$\begin{aligned} E_\Lambda &= (1/2)qJ(J+1) \quad \text{for } e \text{ levels} \\ E_\Lambda &= (1/2)q'J(J+1) \quad \text{for } f \text{ levels,} \end{aligned}$$

where q and q' are defined to be

$$\begin{aligned} q &= 4B^2 \sum_i \frac{|<\Lambda=1|L_+|\Lambda=0;{}^1\Sigma^+(i)>|^2}{E(A^1\Pi)-E({}^1\Sigma^+(i))} \\ q' &= 4B^2 \sum_i \frac{|<\Lambda=1|L_+|\Lambda=0;{}^1\Sigma^-(i)>|^2}{E(A^1\Pi)-E({}^1\Sigma^-(i))}. \end{aligned}$$

From spectroscopic observations of the Λ-doubling, the rotational constant and two Λ-doubling parameters cannot be determined separately. In this investigation, we treated the e- and f-parity states as two separate states, and the effective rotational constants were determined separately for the e- and f-states. Due to the selection rules, the band to the e-levels consists of only P- and R-branch transitions, while the one to the f-levels does of only Q-branch lines. The molecular constants were determined from least squares fittings well, largely because the rotational lines in the ground state were included in the fits. The mass independent parameters have been obtained, and the conventional spectroscopic parameters are derived for each isotopologue. The major molecular constants were determined accurately and were compared with the values obtained previously.

A2

Rotational spectra of water adducts of fluorinated pyridines: Fluorination effects on the interaction topologies

Juan Wang, Xiaolong Li, Gang Feng, Qian Gou
School of Chemistry and Chemical Engineering, Chongqing University, Daxuecheng South Rd. 55,
401331, Chongqing, China.
e-mail: qian.gou@cqu.edu.cn

To get insight into the fluorination effect on the solute molecules, we focused our attention on the water adducts of fluorinated pyridines (PYR). Rotational spectra of the 2,3-difluoropyridine-H_2O, 2,6-difluoropyridine-H_2O and 2,3,6-trifluoropyridine-H_2O complexes have been investigated by using the pulsed jet-Fourier transform microwave technique. Former studies have revealed that water forms a hydrogen bond (HB) to the nitrogen with the oxygen tilted slightly toward either of the *ortho*-hydrogens of the PYR, and a tunneling motion involving in-plane rocking of the water interconverts the resulting equivalent structures.[1] Monofluorination of the *ortho-* and *meta*-hydrogens lead water to link the aromatic ring through an O-H···N HB, while its oxygen is on the opposite side of fluorine, forming a C-H···O weak HB with the adjacent aromatic hydrogen.[2,3] No tunneling splittings have been observed due to the large amplitude motions of water. Extending to the multifluorinated derivatives of PYR, interesting results have been found. The interaction between water and 2,3-difluropyridine has similar topology and internal dynamics as the 2-fluoropyridine-H_2O complex. When both *ortho*-hydrogens are substituted by fluorines, water acts as proton donor forming an O-H···N HB with PYR ring, while the other O-H group tilted to one of the adjacent fluorines. Tunneling splittings were also observed contributable to the internal motion of water. When the third position is further fluorinated, it creates a new active site: water link with 2,3,6-trifluoropyridine through a C-H···O weak HB, acting as a proton acceptor.

References

1. R. B. Mackenzie, C. T. Dewberry, R. D. Cornelius, C. J. Smith, K. R. Leopold. **J. Phys. Chem. A**, *121*, 855-860 (2017).
2. Q. Gou, L. Spada, M. Vallejo-Lopez, S. Melandri, A. Lesarri, E. J. Cocinero, W. Caminati. **ChemistrySelect**, *6*, 1273-1277 (2016).
3. C. Calabrese, Q. Gou, L. Spada, A. Maris, W. Caminati, S. Melandri. **J. Phys. Chem. A**, *120*, 5163-5168 (2016)

A3

Absorption Spectroscopy of H_2O and CH_4 with Amplitude- and Phase-Modulation

Wei-Ling Chen[1], **Tzu-Ling Chen**[1], **Yi-Wei Liu**[1*]
[1]Department of Physics, National Tsing Hua University, Hsinchu, Taiwan, R.O.C.
*Tel: 886-3-574-2561, E-mail: ywliu@phys.nthu.edu.tw

We report on a method of accurate Doppler profile measurement by laser-absorption spectrometry in H_2O and CH_4 molecular. We apply chopped radio frequency to the fiber-EOM as amplitude modulation instead of conventional modulation on light intensity. Producing two far resonant sidebands by fiber-EOM and only one frequency is within the Doppler profile, this approach can increase the signal to noise ratio and eliminate the background noise from laser light intensity. We use 1170 nm laser and multi-pass cell which pushes down the limit of the absorption coefficient α to interact with H_2O and CH_4 molecular. With the result of Doppler width, it may be useful to promote a more precise measurement of the Boltzmann constant k_B in the future.

References

1. C Lemarchand, S Mejri, PLTSow, M Triki, SKTokunaga, S Briaudeau, C Chardonnet, B Darquie, and C Daussy, **A revised uncertainty budget for measuring the Boltzmann constant using the Doppler broadening technique on ammonia**, Metrologia50(2013) 623–630
2. L. Moretti, A. Castrillo, E. Fasci, M. D. De Vizia, G. Casa, G. Galzerano, A. Merlone, P. Laporta, and L. Gianfrani, **Determination of the Boltzmann Constant by Means of Precision Measurements of $H_2{}^{18}O$ Line Shapes at 1.39μm**, PRL111,060803 (2013)
3. G. Casa, A. Castrillo, G. Galzerano, R. Wehr, A. Merlone, D. Di Serafino, P. Laporta, and L. Gianfrani, **Primary Gas Thermometry by Means of Laser-Absorption Spectroscopy: Determination of the Boltzmann Constant**, PRL100,200801 (2008)
4. R. GroBkloB, P. Kersten, and W. Demtriider, **Sensitive Amplitudeand Phase-Modulated Absorption-Spectroscopy with a Continuously Tunable Diode Laser**, Appl. Phys. B 58, 137-142 (1994)

A4

Real-time ion imaging-based rotational/vibrational spectroscopy of nitrogen dimer

Kenta Mizuse[1], **Hikaru Sato**[2], **Genki Ishibashi**[1], **Tomomi Murai**[1],
Haruki Ishikawa[2], **Yasuhiro Ohshima**[1,3]
[1]Department of Chemistry, Tokyo Institute of Technology, Japan
[2]Department of Chemistry, Kitasato University, Japan
[3]Institute for Molecular Science. Japan
mizuse@chem.titech.ac.jp

Nitrogen dimer $(N_2)_2$ is a good model system to study N_2-N_2 interaction, which plays important roles in atmospheric chemistry. There have been, however, only a few, low-resolution spectroscopic studies of $(N_2)_2$ mainly due to its weak dipole moment. In this study, we developed a new method to probe the structure and dynamics of nitrogen dimer by using a time-domain approach. We carried out impulsive Raman excitation pump and Coulomb-explosion-imaging probe experiment. Because dipole transitions of nitrogen dimer would be weak, we focused on the Raman process. Imaging probe gives us instantaneous structural/spatial information. From the observed period of image parameters, rotational/vibrational frequencies can be deduced. In the experiment, $(N_2)_2$ formed in a supersonic jet expansion were irradiated with a linearly polarized Raman pump pulse (820 nm, <1 ps, 0.5 mJ). Subsequent dynamics were probed with a time-delayed, circularly polarized probe pulse (407 nm, 80 fs, 0.3 mJ). Upon probe irradiation, $(N_2)_2$ was doubly ionized, and N_2^+ fragments were ejected due to the Coulomb repulsion. Spatial distribution of the N_2^+ fragments was measured with a newly developed 2D spatial-slice ion imaging setup.[1]

Figure 1 shows the time-dependent orientation function of $(N_2)_2$ obtained from the observed real-time image. When the intermolecular axis of the dimer is oriented along the pump pulse polarization, the value of this function becomes larger. Therefore, the time trace corresponds to the time-domain rotational spectroscopic data. In this trace, revival structures with a ~230 ps period can be seen. This period corresponds to $2B$, where B is the rotational constant. From this spectroscopic data, the intermolecular distance of the nitrogen dimer was estimated to be 407.9 pm. Details of our new experimental setup and analyses of spectral data will be presented.

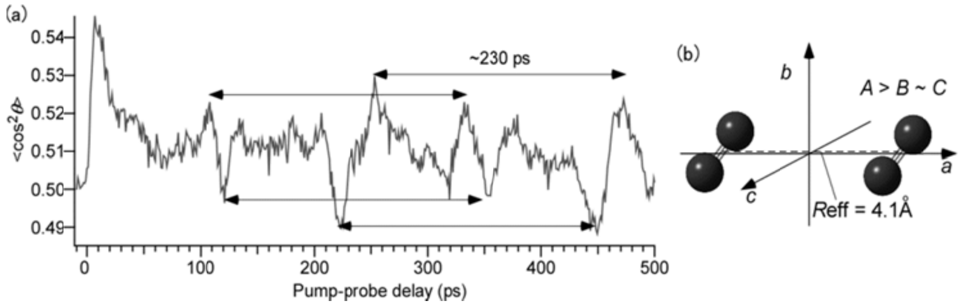

Figure 1. (a) Time trace of the orientation function $<\cos^2\theta>$, where θ is the ejected angle of the N_2^+ ions with respect to the pump polarization. (b) Schematic of nitrogen dimer shown with the experimentally obtained intermolecular distance.

References

1. K. Mizuse, K. Kitano, H. Hasegawa, Y. Ohshima, **Sci. Adv**. *1*, e1400185 (2015).

A5

New electronic states of YO in the UV region

Allan S-C. Cheung[1], Na Wang, Y. W. Ng[1], Andrew Clark[1] and Wenli Zou[2]

[1]Department of Chemistry, The University of Hong Kong, Hong Kong, Pokfulam Road, Hong Kong

[2]Institute of Modern Physics, Northwest University, Xi'an, China and Shaanxi Key Laboratory for Theoretical Physics Frontiers, Xi'an, Shaanxi, China

Email: hrsccsc@hku.hk

Laser excitation spectra of the yttrium monoxide (YO) molecule in the ultra violet region between the 280 and 320 nm have been recorded and studied using optical-optical double resonance (OODR) spectroscopy. The YO molecule was prepared by the reaction of laser ablated yttrium atom with oxygen under supersonic jet cooled conditions. Thirteen vibration bands have been observed via the intermediate $B^2\Sigma^+$ state from the $X^2\Sigma^+$ state. The excited states analyzed so far are generally in good case (c) coupling scheme. Besides the observation of excited $\Omega = 0.5$ and 1.5 sub-states, and $^2\Sigma^+$ state, we have also identified and studied a forbidden transition, the [33.7] $^4\Sigma^-$ - $B^2\Sigma^+$ transition. Molecular constants for the newly observed electronic states were determined by least squares fitting the measured rotational lines.

A number of low-lying Λ-S states and Ω sub-states of the YO molecule have been calculated using SA-CASSCF (state-averaged complete active space self-consistent field) followed by MS-CASPT2 (multi-state complete active space second-order perturbation theory). Since the active Y 5p shell is very important to get some low-lying electronic states with the correct principal configurations, the active space consists of 7 electrons in 12 orbitals corresponding to the Y 4d5s5p and O 2p shells. The molecular orbitals from Y 4s4p and O 2s are inactive but are also correlated, whereas the lower core-shells are relaxed only by SA-CASSCF and then kept frozen at the CASPT2 level. Spin-orbit coupling (SOC) is treated via the state-interaction (SI) approach with the one-center atomic mean field integral (AMFI) approximation for one- and two-electron spin-orbit integrals. In the SOC calculations of potential energy curves (PECs), the SA-CASSCF wavefunctions are adopted where the diagonal elements in the SOC matrix are replaced by the corresponding MS-CASPT2 energies calculated above. A comparison of the spectroscopic properties of electronic states determined experimentally and from calculations will be presented.

A6

Low-lying electronic states of Scandium monocarbide, ScC, observed by laser-induced fluorescence

Chiao-Wei Chen, Anthony J. Merer and Yen-Chu Hsu
Institute of Atomic and Molecular Sciences, Academia Sinica, P.O. Box 23-166, Taipei 10716, Taiwan.
e-mail: cwchen@pub.iams.sinica.edu.tw, merer@chem.ubc.ca, ychsu@po.iams.sinica.edu.tw

Scandium carbide molecules (ScC) have been prepared by the reaction of laser-ablated scandium metal with acetylene under supersonic jet-cooled conditions. Rotational analyses of excitation spectra of $Sc^{12}C$ and $Sc^{13}C$ in the region 14000 – 16000 cm^{-1} have shown that four low-lying electronic levels are populated, one with $\Omega'' = 5/2$, two with $\Omega'' = 3/2$ and one with $\Omega'' = 1/2$. Wavelength-resolved emission spectra show that the lowest-lying level is an $\Omega'' = 3/2$ level, with an $\Omega'' = 1/2$ level lying 42 cm^{-1} higher; these two levels are assigned as the spin-orbit components of a $^2\Pi_i$ electronic state. The other two observed levels are spin-orbit components of a metastable $^4\Pi_i$ state ($a^4\Pi_{5/2}$ and $a^4\Pi_{3/2}$), lying respectively 155 and 174 cm^{-1} above the $^2\Pi_{3/2}$ ground state. The ground state bond length is 1.952 (1) Å, and the vibrational frequencies in $Sc^{12}C$ and $Sc^{13}C$ are 648 (2) and 631 (2) cm^{-1}, respectively. For the $a^4\Pi$ state, the bond length is 1.924 (10) Å and the vibrational frequencies of the two isotopomers are 711 (2) and 692 (2) cm^{-1}. Strong doublet-quartet mixing is evident in many of the excited electronic states of the 14000 – 16000 cm^{-1} region, which results in some complicated patterns of bands. Among the observed excited states are two $^4\Delta_r$ states.

A7

Spectroscopy of the B(1)-X(0^+) transitions of PbO with 10-MHz precision and control of the translational motion with a microwave field

Katsunari Enomoto
Department of Physics, Faculty of Science, University of Toyama
enomoto@sci.u-toyama.ac.jp

We have performed high precision spectroscopy of PbO molecules [1]. The B(1)(v’=3-6)—X(0^+)(v”=0) transitions located in 398-423 nm were investigated by using a cold and slow PbO beam generated by laser ablation and cryogenic helium buffer-gas cooling. About 140 lines were measured by comparing with resonances of an ultralow expansion etalon. The etalon has small group-delay-dispersion mirrors to be an accurate frequency reference over a wavelength span of a few tens of nanometer [2]. This system shown in Fig. 1 allows us to determine absolute frequencies of the observed PbO lines with the uncertainty of about 10 MHz. The spectroscopic constants of the B(1) state were precisely determined.

We found that the v’=4 state is considerably perturbed. For example, the rotational constant *B* does not follow the usual reduced mass dependence among the isotopologues. The v’=4 levels are well reproduced by assuming a homogeneous perturbation due to a vibronic state, which is expected to be the a(1) v’=19 state.

We are also pursuing the control of the translational motion of polar molecules using an intense microwave standing wave in superconducting resonators. Focusing, deceleration, and trapping of molecules in high-field-seeking states, which have a lower energy at a higher electric field, can be realized by the use of such intense microwave. We have shown that a Pb-Sn coated copper resonator at about 3 K has a high quality factor of 10^6 and tolerates several watts of input power [3]. The current status of this project will also be presented in this talk.

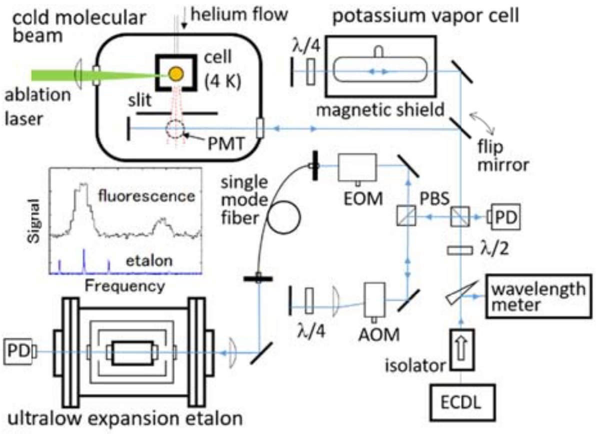

Fig 1: Experimental setup for spectroscopy

References

1. K. Enomoto, A. Fuwa, N. Hizawa, Y. Moriwaki, and K. Kobayashi, **J. Mol. Spectrosc.**, 339, 12-16 (2017).
2. K. Enomoto, N. Hizawa, T. Suzuki, K. Kobayashi, and Y. Moriwaki, **Appl. Phys. B**, 122, 126 (2016).
3. K. Enomoto *et al.*, **Appl. Phys. B**, 109, 149-157 (2012).

A8

Substituent effect on electronic transition energy of multi methyl-substituted benzyl radicals

Sang Kuk Lee
Department of Chemistry, Pusan National University, Busan 46241, South Korea
sklee@pusan.ac.kr

Transient species such as molecular radicals and ions have been believed to play an important role as intermediates in chemical reactions. The structure and characteristics of transient species provide clear understanding for definitions of the properties of chemical reactivity in reaction dynamics.

Ring-substituted benzyl radicals always exhibit electronic energies of the $D_1 \rightarrow D_0$ transition being shifted to red region with respect to the parental benzyl radical. The effect of methyl substitution on the electronic transition is strongly dependent on the number, and position of methyl substituents. The red-shifts have been measured from the visible vibronic emission spectra observed from corona discharge of methyl-substituted benzene precursors in a technique of corona excited supersonic expansion (CESE) which has been developed in this laboratory over the past 20 years. By analyzing the red-shifts of di-, tri-, and tetra-methyl substituted benzyl radicals with variation of substitution positions, a simple but very useful model[a] has been established to predict the size of red-shifts quantitatively. In the model based on the Hückel's molecular orbital theory, the position of mode and wave amplitude at the lowest unoccupied molecular orbitals (LUMO) can explain the variation of the red-shifts for the emission scheme.

In the presentation, a table lists the positions of origin band in the $D_1 \rightarrow D_0$ transition as well as the amount of red-shift for methyl-substituted benzyl radicals collected from the vibronic emission spectra observed for each species. The model developed in this work will be also discussed for the description of the variations of the red-shifts with the position and the number of methyl substitution.

1. Y. W. Yoon, S. Y. Chae, S. K. Lee, **Chem. Phys. Lett.**, *644*, 167-170 (2016).

A9

Microwave Study of Internal Rotation in *p*-Tolualdehyde: Local versus Global Symmetry at the Methyl-Rotor Site

H. Saal[a], J.-U. Grabow[a], A.R. Hight Walker[b], J.T. Hougen[b], I. Kleiner[c], W. Caminati[d]
[a] G.-W.-Leibnitz-Universität, Institut für Physikalische Chemie und Electrochemie, Callinstrasse 3A, D-30167 Hannover, Germany
[b] NIST, Gaithersburg, MD 20899-8441, USA.
[c] Laboratoire Interuniversitaire des Systèmes Atmosphériques, CNRS et Universités Paris, 61 av Général de Gaulle, 94010, Créteil, France
[d] Universitá di Bologna, Dipartimento de Chimica "G. Ciamician," via F. Selmi 2, 40126 Bologna, Italy
e-mail: jon.hougen@nist.gov

The rotational spectrum of *para*-tolualdehyde (CH_3-C_6H_4-CHO) has been measured using microwave spectrometers in three laboratories, with the goal of quantifying the influence of the aldehyde group at the top of the benzene ring on the internal rotation barrier seen by the methyl group at the bottom of the ring. This barrier consists of a six-fold component, which results from the local C_{2v} symmetry of the benzene ring seen by the methyl top (as in toluene), and an additional three-fold component, which results from information on the non-C_{2v} symmetry at the aldehyde site being transmitted across the ring to the methyl top site.

The nearly free internal rotation of the methyl group splits each of the rotational transitions into two components, one of *A* and one of *E* symmetry. Assignment and fit of 786 *A*-state and *E*-state transitions to an internal rotation Hamiltonian with centrifugal distortion and barrier terms of three-fold (V_3 = 28.111(1) cm^{-1}) and six-fold (V_6 = -4.768(7) cm^{-1}) symmetry with respect to the internal rotation angle, resulted in residuals equal to experimental uncertainty. Isotopic data from all eight mono-substituted ^{13}C isotopologs and the one ^{18}O isotopolog were obtained in natural abundance and used to determine an r_s substitution structure.

Various chemical and physical implications of this structure and the two barriers will be discussed, in connection with ab initio calculations available in the NIST Computational Chemistry Comparison and Benchmark Data Base. In particular, our initial intuitive assumption that the information transmission mechanism would involve a conjugation of the π electrons of the aldehyde C=O with the π electrons of the benzene ring to force a partial Kekulé structure of the ring, is not supported by the quantum chemistry calculations.

A10

Hyperfine Splittings of Methanol in the First Torsional State

Li-Hong Xu[a], J.T. Hougen[b], G.Yu. Golubiatnikov[c], S.P. Belov[c], A.V. Lapinov[c], E.A. Alekseev[d,e], I. Krapivin[d], L. Margulès[f], R. A. Motiyenko[f], S. Bailleux[f]

[a] Department of Physics and CLAMS, University of New Brunswick, Saint John, NB, E2L 4L5, Canada (lxu@unb.ca)

[b] Sensor Science Division, NIST, Gaithersburg, MD 20899-8441, USA.

[c] Institute of Applied Physics of RAS, 603950 Nizhny Novgorod, Russia.

[d] Institute of Radioastronomy of NASU, 61002 Kharkov, Ukraine.

[e] Quantum Radiophysics Department of V.N. Karazin Kharkiv National University, Svobody Square 4, 61022, Kharkov, Ukraine.

[f] Laboratoire PhLAM, Université de Lille1, Lille, France.

Hyperfine splittings in the ground state of CH_3OH have recently been studied by several groups [1,2,3]. In our work [2], we treated splittings in the Lamb-dip sub-mm-wave transitions between some torsion-rotation states of E symmetry. These doublets increase nearly linearly with J, and we attributed them to the effect of torsionally mediated spin-rotation interaction of the methyl protons [2]. Hyperfine doublets of this type have so far been observed only in methanol. The focus of this talk is on hyperfine doublet, triplet and quartet splittings observed in the first excited torsional state of CH_3OH. Four series of lines with successive J values dominate the available data, with measurements from three laboratories: Nizhny Novgorod in Russia, Kharkov in the Ukraine, and Lille in France. These four $v_\tau = 1$ series of E-species transitions are:

1. from Kharkov/Lille, $K = 6 \leftarrow 7$, Q branch quartets, with $7 \leq J \leq 15$;
2. from NNOV, $K = 3 \leftarrow 2$, Q branch, with $3 \leq J \leq 18$, where the series starts as quartets, changes to doublets at $J = 7$, and then finally to singlets at $J = 17$;
3. from NNOV, $K = -2 \leftarrow -3$, P branch doublets, with $8 \leq J \leq 12$;
4. from Kharkov/Lille, $K = 8 \leftarrow 7$, Q branch, with $8 \leq J \leq 24$, where the series starts as triplets and becomes doublets at $J = 15$. We have ignored the central features of the triplets, since they might be due to unusual double-N crossover resonances.

We have empirically modeled the hyperfine splittings of these four series with spin-torsion and spin-rotational terms for the two $I = ½$ spin systems arising from the OH and CH_3 protons, respectively. Work is in progress to untangle eight different contributions to the empirical fitting constants. In addition, we are trying to fit a few isolated measurements (that do not fall into long series).

References:

[1] L. H. Coudert, C. Gutle, T. R. Huet, J.-U. Grabow, S. A. Levshakov, “Spin-torsion effects in the hyperfine structure of

methanol”, J. Chem. Phys. 143 (**2015**) 044304.

[2] S.P. Belov, G.Yu. Golubiatnikov, A.V. Lapinov, V.V. Ilyushin, E.A. Alekseev, A.A. Mescheryakov, J.T.Hougen, Li-Hong Xu, J. Chem. Phys. 145 (**2016**) 024307.

[3] Boy Lankhaar, Gerrit C. Groenenboom, and Ad van der Avoird. “Hyperfine interactions and internal rotation in methanol”, J. Chem. Phys. 145 (**2016**) 244301.

A11

Microwave Zeeman Effect of Methanol

Kojiro Takagi[a], Shozo Tsunekawa[a], Kaori Kobayashi[a], Tomoya Hirota[a], and Fusakazu Matsushima[a]

[a] Department of Physics, University of Toyama, 3190 Gofuku, Toyama 930-8555, Japan

[b]National Astronomical Observatory of Japan and SOKENDAI (The Graduate University for Advanced Studies), Osawa 2-21-1, Mitaka, Tokyo 181-8588, Japan

kaori@sci.u-toyama.ac.jp

Splittings between right- and left-circular polarizations of methanol maser transitions have been observed in star-forming regions at several frequencies (6.7 GHz etc.) [1, 2]. If the splitting is caused by the Zeeman effect, it is possible to deduce magnetic field strength in these regions. Magnetic field is considered to be an important factor related to star formation. To determine this magnetic field from the splittings, it is essential to use laboratory data of the Zeeman effect of methanol (or, its g-factor).

As a preliminary laboratory study on the Zeeman effect of methanol, Zeeman splittings of a series of Q-branch transitions in the 25 GHz range were observed [3]. These splittings were applied to determine the Zeeman splitting coefficients of the maser transitions. This treatment is not appropriate, and we started laboratory measurements of methanol transitions to determine g-factor coefficients so that the Zeeman splittings of any transitions can be calculated.

The splitting of the singlet sigma molecule is small and strong magnetic field is required to observe such transitions. Neodymium magnets are used to produce about 0.7 T magnetic field. A conventional source-modulation spectrometer combined with waveguide cells were used to observe splittings of methanol. Splittings of many transitions including torsional excited state were successfully observed. The effective g-factor were obtained. We will report the current status.

References

1. W. H. T. Vlemmings, **Proc. IAU Symposium**, *287*, 31 (2012).
2. A. P. Sarma, **Proc. IAU Symposium**. *287*, 41 (2012).
3. C .K. Jen, **Phys. Rev.** *81*, 197 (1951).

A12

Dimers of hydrofluoroalkanes by microwave spectroscopy

Xiaolong Li, Junhua Chen, Tao Lu, Qian Gou, Gang Feng
School of Chemistry and Chemical Engineering, Chongqing University, Daxuecheng South Rd. 55,
401331 Chongqing, China
e-mail: fengg@cqu.edu.cn

Hydrofluoroalkanes are prototype molecules for investigating the nature of C–H···F–C hydrogen bond. The degree of fluorine substitution and the carbon skeleton length of this class of compounds may significantly affect the molecular properties of the monomers and therefore alter their complexation behavior. We investigated the dimers of several hydrofluoroalkanes in gas phase by pulsed jet Fourier transform microwave spectroscopy and theoretical calculations. We present here the structure, conformational equilibrium and C–H···F–C hydrogen bonds of 1,1,1,2-tetrafluoroethane dimer, 1,1-difluoroethane dimer, 1,1,1,2-tetrafluoroethane–difluoromethane dimer and 1,1-difluoroethane–difluoromethane dimer.

For 1,1,1,2-tetrafluoroethane dimer, one conformer stabilized through a network of four C–H···F–C interactions was observed. The measurements, extended to four ^{13}C species in natural abundance, allowed determination of the carbon skeleton structures and evaluation of the weak hydrogen bond parameters.

For 1,1,-difluoroethane dimer, two most stable isomers have been detected, which are both stabilized by a network of three C–H···F–C weak hydrogen bonds. For the global minimum, the measurements have also been extended to its four ^{13}C isotopologues in natural abundance, allowing a precise structural determination.

Three conformers were observed for 1,1,1,2-tetrafluoroethane–difluoromethane dimer and 1,1-difluoroethane–difluoromethane dimer, respectively. The structures and conformational preferences of these two dimers were also provided.

References

1. X. Li, Y. Zheng, J. Chen, J. U. Grabow, Q. Gou, Z. Xia, G. Feng, **J. Phys. Chem. A** *121*, 7876-7881 (2017).
2. J. Chen, Y. Zheng, J. Wang, G. Feng, Z. Xia, Q. Gou, **J. Chem. Phys**. *147*, 094301 (2017).

A13

Simulation of realistic vibrational spectra line-shapes: anharmonic effects on the band position and transition intensities

Malgorzata Biczysko[1]**, Julien Bloino**[2]
[1]International Center for Quantum and Molecular Structures, Shanghai University, Shanghai, China
[2]ICCOM-CNR, UOS Pisa, Italian National Research Council, Pisa, Italy
e-mail: biczysko@i.shu.edu.cn

An accurate comparison between simulated and experimental vibrational spectra requires going beyond the double-harmonic approximation, including anharmonic effects on vibrational energies, as well as on intensities. While the former are independent of the spectroscopy, the latter can only be done through property- and transition-specific developments, ideally taking into account the anharmonicity of both wave function and properties. This results in a proper account of the intensity of non-fundamental transitions and more accurate band-shapes. Recent developments on a comprehensive and robust generalized version of the second-order vibrational perturbation theory (GVPT2) for vibrational averages and transition properties have made possible the simulation of fully anharmonic infrared (IR), Raman spectra, as well as their chiral counterparts, namely vibrational circular dichroism (VCD) and Raman optical activity (ROA), for medium-to-large molecular systems [1,2]. We will show that a very good agreement between computed and experimental spectra, considering both band positions and their relative intensities, which define the overall spectral pattern, can be achieved for closed- and open-shell medium size semi-rigid molecular systems [1-4] also in the regions dominated by non-fundamental transitions [4].

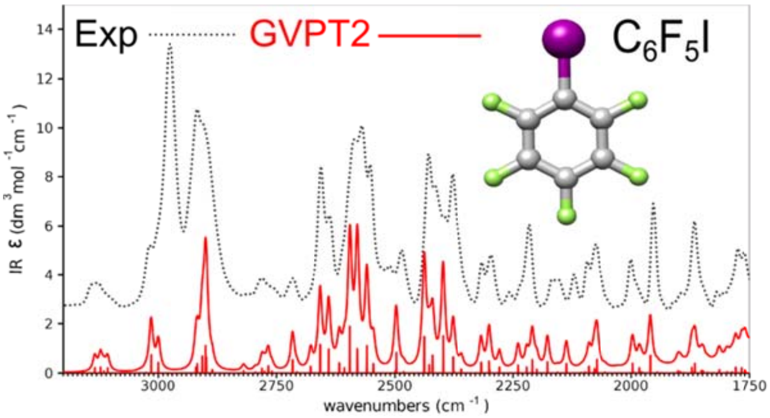

References

1. J. Bloino, M. Biczysko, V. Barone, **J. Phys. Chem. A**, *119*, 11862 (2015)
2. J. Bloino, A. Baiardi, M. Biczysko, **Int. J. Quant. Chem.** *116*, 1543 (2016)
3. M. Biczysko, J. Bloino, C. Puzzarini, **WIREs Comput Mol Sci** doi: 10.1002/wcms.1349 (2017)
4. M. H. Palmer, M. Biczysko, K.A. Peterson, C.S. Stapleton, S.P. Wells, **J. Phys. Chem. A** *121*, 7917 (2017)

A14

Theoretical study on the vibrational states for HO_3 system based on full-dimensional potential energy surface

Xixi Hu,[1] **Hua Guo**,[2] **and Daiqian Xie**[1]

[1] Institute of Theoretical and Computational Chemistry, Key Laboratory of Mesoscopic Chemistry, School of Chemistry and Chemical Engineering, Nanjing University, Nanjing 210023, China

[2] Department of Chemistry and Chemical Biology, University of New Mexico, Albuquerque, New Mexico 87131, USA
e-mail: xxhu@nju.edu.cn, dqxie@nju.edu.cn

To provide a deeper understanding of HO_3 system, the vibrational energy levels of hydrogen trioxy radical (HO_3) were calculated based on a newly developed potential energy surface (PES) using the exact vibrational Hamiltonian and the Lanczos algorithm. The new six-dimensional PES has been constructed by fitting to 2087 energy points for the electronic ground-state of HO_3 (X^2A'') using the permutation invariant polynomial-neural network (PIP-NN) approach. The energy points are calculated using MRCI-F12/cc-pVDZ-F12 method including Davidson corrections using rotated reference energies.

The PES shows that the trans-HO_3 isomer is the global minimum with a potential well depth of 4.790 kcal/mol with respect to the OH+O_2 asymptote. The equilibrium geometry of the cis-HO_3 conformer is located 0.173 kcal/mol above that of the trans-HO_3 with an isomerization barrier of 1.055 kcal/mol from trans-HO_3. For the trans-HO_3, the middle O_2O_3 bond length (1.6584 Å), is slightly shorter than the commonly accepted value of 1.688 Å[1] but larger than the predicted value (≤1.61 Å) from CCSD(T) calculations.[2]

Based on this PES, a rigorous quantum dynamics study has been carried out for computing the rovibrational energy levels of HO_3. The calculated fundamental frequencies of HO_3 and DO_3 are in good agreement with the experimental values obtained by Derro et al.[3] using IR-UV double resonance technique. Because of the strong intermodal coupling and the low-frequency torsional mode, the calculation of the highly excited vibrational spectra of HO_3 are known to be notoriously difficult. Our calculations yielded some vibrational levels above the ground vibrational levels. Some low-lying levels were assigned with six normal mode quantum numbers.

References

1. K. Suma, Y. Sumiyoshi, Y. Endo, **Science**, *308,* 1885 (2005).
2. A.J.C. Varandas, **J. Chem. Theory Comput.**, *8,* 428 (2012).
3. E.L. Derro, T.D. Sechler, C. Murray, M.I. Lester, **J. Chem. Phys.,** *128*, 244313 (2008).

A15

The vibrational levels of the Ã state of C_3Ar studied by hole-burning experiments and ab initio calculations

Yi-Jen Wang and **Yen-Chu Hsu**
Institute of Atomic and Molecular Sciences, Academia Sinica,
P. O. Box 23-166, Taipei 10617, Taiwan
e-mail: edith043@gmail.com, ychsu@po.iams.sinica.edu.tw

In the range of 25025-25520 cm^{-1}, 14 vibrational bands of the Ã state of C_3Ar have been studied using laser-induced fluorescence techniques.[1] Among them, six vibrational bands are rotationally resolved or partially resolved.[2] The emission spectra of these 14 bands suggest that two types of predissociation processes are occurring, distinguished by different vibrational energy distributions of the C_3 fragments. One follows the energy gap law closely, but the other does not. A hole-burning experiment has been carried out to confirm that 9 of the bands originate from the ground vibrational level of $C_3Ar(\tilde{X})$, not from hot bands or other van der Waals (vdW) complexes. Rotational contour analysis of the hole-burning spectra also suggests that, where the bands occur in pairs, one member is a type A band and the other is a type C band, with the type A band to the red of the type C band. The vdW vibrational frequencies and equilibrium geometry of the Ã state of C_3Ar have been calculated at the level of RS2/cc-pVTZ. The hole-burning experiments and the results of the ab initio calculations will be presented.

References

1. Guiqiu Zhang, Bon-Gi Lin, S.-M. Wen, and Yen-Chu Hsu, J. Chem. Phys. **120**, 3189-3200 (2004).
2. Anthony J. Merer, Yen-Chu Hsu, Yi-Ren Chen, and Yi-Jen Wang, J. Chem. Phys. **143**, 194304(2015).

A16

Halogen Molecular Elimination from Halogen-containing Compounds in Atmosphere Using Cavity Ring-down Spectroscopy

King-Chuen Lin
Department of Chemistry, National Taiwan University, Taipei, and Institute of Atomic and Molecular Sciences, Academia Sinica, Taipei 106, Taiwan
kclin@ntu.edu.tw

Atmospheric halogen chemistry has drawn much attention, for the halogen atom (X) playing a catalytic role may cause severe stratospheric ozone depletion. X atomic elimination from X-containing hydrocarbons is recognized as the major primary dissociation process upon UV-light irradiation, whereas a direct elimination of X_2 product has been seldom discussed or remained as a controversial issue. This talk will cover the detection of X_2 primary products using cavity ring-down absorption spectroscopy in the photolysis at 248 nm of a variety of X-containing compounds, focusing on bromomethanes, dibromoethanes, dibromoethylenes (1,1-$C_2H_2Br_2$ and 1,2-$C_2H_2Br_2$), diiodomethane, thionyl chloride ($SOCl_2$), along with acyl bromides (BrCOCOBr and $CH_2BrCOBr$). The optical spectra, quantum yields, and vibrational population distributions of the Br_2, I_2, and Cl_2 fragments have been characterized. With the aid of *ab initio* calculations of potential energies and rate constants, the detailed photodissociation mechanisms may be comprehended. Such studies are fundamentally important to gain insight into the dissociation dynamics and may also practically help to assess the halogen-related environmental issues.

References

1. C. C. Wu, H. C. Lin, Y. B. Chang, P. Y. Tsai, Y. Y. Yeh, H. Fan, K. C. Lin, and J. S. Francisco, **J. Chem. Phys.**, *135*, 234308 (2012).
2. K. C. Lin and P. Y. Tsai, **Phys. Chem. Chem. Phys. (Perspective)**, *16*, 7184(2014).
3. B. J. Chen, P. Y. Tsai, T. K. Huang, Z. H. Xia, K. C. Lin, C. J. Chiou, B. J. Sun, and A. H. H. Chang, **Phys. Chem. Chem. Phys.**, ***17***, 7838 (2015).
4. T. K. Huang, B. J. Chen, K. C. Lin, L. Lin, B. J. Sun, and A. H. H. Chang, **J. Phys. Chem. A,** *121*, 2888 (2017).

A17

Dependence of Proton-Transfer Dynamics on the Configuration of Diols as Effective Brønsted Bases

Ye-Jin Kim[a, b], **Jae-Heon Park**[a, b], **Hak-won Nho**[b] **and Oh-Hoon Kwon**[a, b*]
[a]Center for Soft and Living Matter, Institute for Basic Science (IBS), [b]Department of Chemistry,
School of Natural Science, Ulsan National Institute of Science and Technology (UNIST)
e-mail: ohkwon@unist.ac.kr

As viscous hydroxylic organic compounds, diols are of interest for their functional molecular conformation, which is based on inter- and intramolecular hydrogen (H)-bonds. By utilising steady-state electronic and vibrational spectroscopy, time-resolved fluorescence spectroscopy, and computational analyses, we report the association of the hydroxyl groups of diols via intra- or intermolecular H-bonds to enhance their reactivity as a base. Whereas the formation of an intermolecularly H-bonded dimer is requisite for diols of weak intramolecular H-bond to extract a proton from a model strong photoacid, a well-configured single diol molecule having an optimised intramolecular H-bond is revealed to serve as an effective Brønsted base with increased basicity, which was evidenced by quantum chemical calculations, where the proton-transfer rate for the well-configured H-bonded complex is revealed to correlate well with the intramolecular H-bond length of a H-bond wiring diol molecule. This observation highlights the collective role of H-bonding in acid-base reactions, and provides mechanistic backgrounds to understand the reactivity of polyols in the acid-catalysed dehydration for the synthesis of cyclic ethers at the molecular level.

A18

Excited-State Proton-Transfer Dynamics of 6-Hydroxyquinoline with Amphiprotic Weak Acid in a Nonpolar Liquid Phase Solvent

Kyeong-Eun Mun, Won-Woo Park, Oh-Hoon Kwon*
Department of Chemistry, Ulsan National Institute of Science and Technology (UNIST), Ulsan 44919, Republic of Korea
e-mail: ohkwon@unist.ac.kr

In proton relay, a single hydroxyl group, *e.g.*, of water or alcohol, generally acts as both a proton donor, a protic hydrogen (H), and an acceptor, non-bonding electrons on the oxygen atom, simultaneously. In this sense carboxylic acid is unique as a proton-relaying amphiprotic compound because it has the acidic and basic functionality at different sites: hydroxyl and carbonyl groups, respectively. By stabilizing/destabilizing transition (or intermediate) states of the proton-relaying entity, this structural difference may affect the reaction path, resulting in the bifurcation of the proton-diffusion mechanism via either Grotthuss- or Brownian-type behavior.

To investigate the pattern of proton relay via carboxylic acid we chose the prototype system, 6-hydroxyquinoline (6HQ), which can form H-bonded complexes with protic guest molecules, acetic acid (AcOH) in this study [1]. Upon photoexcitation 6HQ is well known to undergo fast prototropic tautomerization via excited-state proton transfer (ESPT) when the acidic hydroxyl and basic imine functional groups of 6HQ are H-bond bridged by guest protic molecules [2].

From the steady-state spectroscopic measurements we found that 6HQ forms complexes with AcOH in 1:1 and 1:2 stoichiometry. When 6HQ is complexed with two AcOH molecules, 6HQ is observed to accept a proton from the AcOH dimer in the ground state to transform into a cationic form. When such the cation is electronically excited, time-resolved fluorescence measurements revealed that ESPT took place consecutively to give birth to a keto species with a proton being released at the imine site on the timescales of 10’s and 100’s ps. On the other hand, the prototropic tautomerization seems not to occur when the 1:1 complex of 6HQ-AcOH was photoexcited, because a single AcOH molecule cannot H-bond bridge the imine and enol groups of 6HQ. The detailed reaction mechanisms will be discussed in the presentation.

References

1. M. S. Mehata, **J. Phys. Chem. B**, *112*, 8383-8386 (2008).
2. T. G. Kim, Y. Kim and D.-J. Jang, **J. Phys. Chem. A**, *105*, 4328-4332 (2001).

A19

Study on Nonradiative Decay and Photoisomerization Route of Cinnamic Acid Derivatives

T. Ebata[*1], **S. Kinoshita**[1], **Y. Inokuchi**[1], **H. Kohguchi**[1], **N. Akai**[2], **M. Ehara**[3,4], **K. Yamazaki**[5], **Y. Harabuchi**[6,7], **S. Maeda**[6], **T. Taketsugu**[6]
[1]Graduate school of Science, Hiroshima University, [2]Graduate school of BASE, Tokyo University of Agriculture and Technology, [3]IMS, [4] SOKENDAI, [5]Institute of Materials Research, Tohoku University, [6]Graduate school of Science, Hokkaido University, [7]JST-Presto
*e-mail: tebata@hiroshima-u.ac.jp

The nonradiative decay (NRD) route leading *trans* → *cis* isomerization after the photo-excitation to $S_1(\pi\pi^*)$ has been investigated for several cinnamate derivatives. They exist as a chromophore of PYP and lignin in plants in nature, and are also known as sunscreen cosmetic reagents. However, the detail of the photoisomerization mechanism has not been understood yet. In the present study, we investigated the structural isomers of hydroxy-methylcinnmate (HMC, Fig.1): *ortho*-, *meta*-, and *para*-HMC to elucidate the substitution effect on the NRD and isomerization routes. In addition, we investigated the effect of complexity of the ether group such as *para*-methoxy-methyl, -ethyl and -2ethylhexyl cinnamate (*p*-MMC, *p*-MEC, *p*-M2EHC).

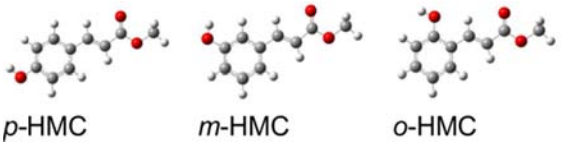

Fig.1 Structural isomers of HMC

Experimentally, we measured the S_1-S_0 electronic spectra and the S_1 lifetimes to investigate the excess energy dependence of the S_1 lifetime for supersonically-cooled gas phase molecules. We also observed a transient state produced after the decay of S_1, by nanosecond UV- deep UV pump-probe spectroscopy and determined the energy from S_0. In addition to the gas phase study, we measured photo-product after uv irradiation by using cold matrix FTIR spectroscopy.

The experimental results are compared with theoretical calculation for the excited states and decay routes based on GRRM theory with TDDFT calculation. From these results, we concluded the isomerization mechanism is different between *p*-HMC and *o*- and *m*- HMC: *p*-HMC undergoes [$S_1 \rightarrow {}^1n\pi^* \rightarrow T_1 \rightarrow$ isomerization] route. On the other hand, *o*- and *m*- HMC undergo [$S_1 \rightarrow$twisting along C=C double bond to ~90 degrees in $S_1 \rightarrow$internal conversion to S_0 and isomerize to *cis*-form].

If I have time, we will describe our new laser ablation/supersonic jet setup for laser spectroscopy of nonvolatile molecules and their hydrated complexes.

References

1. D. Shimada et al., *Phys. Chem. Chem. Phys.*, **14**, 8999–9005 (2012)
2. Y. Miyazaki et al., *J. Chem. Phys.*, **141**, 244313 (13 pages) (2014)
3. Y. Miyazaki et al., *J. Phys. Chem. Lett.*, **6**, 1134-1139 (2015)
4. K. Yamazaki et al., *J. Phys. Chem. Lett.*, **7**, 4001−4007 (2016)

B1

Ultrahigh-resolution spectroscopy of polycyclic aromatic hydrocarbons

Masaaki Baba
Graduate School of Science, Kyoto University, Japan
baba@kuchem.kyoto-u.ac.jp

Polycyclic aromatic hydrocarbons (PAHs) are of great interest to investigate the molecular structure and excited-state dynamics. We observed the rotationally resolved ultrahigh-resolution spectra of electronic transitions for several planar PAHs. The experimentally obtained rotational constants can be examined by comparing with the results of theoretical calculation, providing the approximate geometrical structure of the isolated molecule.

Polycyclic Aromatic Hydrocarbons (planar)

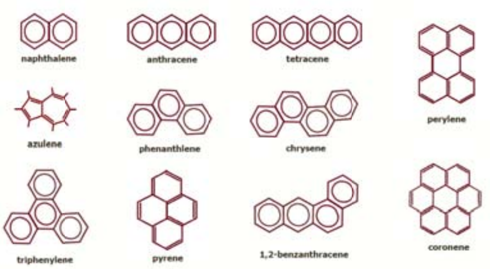

For benzene,[1] naphthalene,[1] anthracene,[2] phenanthrene,[3] pyrene,[4] and perylene,[5] we could observe high-quality spectra, and determined accurate rotational constants. The experientially obtained rotational constants at the S_0 zero-vibrational level are in very good agreement with those obtained by ab initio theoretical calculation (MP2/6-31G(d,p)) for four significant figures. The calculated molecular structure is therefore considered to be approximately true.

(a) Ultrahigh-resolution spectrum of naphthalene and (b) simulation.

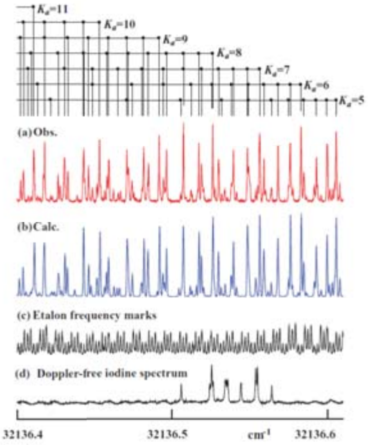

In contrast, the theoretical calculation does not work well for the electronic excited state. We have to elucidate the excited-state dynamics by analyzing the ultrahigh-resolution spectrum much more in detail. Recently, we found that the fluorescence lifetime was dependent on rotational levels in the S_0 high vibrational level of naphthalene. It is considered that intramolecular vibrational redistribution (IVR) by Coriolis interaction enhances internal conversion (IC) to the S_0 state. Intersystem crossing (ISC) to the triplet states is considered to be slow in planar PAHs.[6] Now we are challenging other planar PAHs.

References

1. M. Baba, T. Ishimoto, U. Nagashima, et al., **J. Chem. Phys.** *135*, 054305 (2011)
2. M. Baba, N. Nakayama, T. Ishimoto, et al., **J. Chem. Phys.** *130*, 134315 (2009)
3. Y. Kowaka, M. Baba, and T. Yamanaka, **J. Chem. Phys.** *136*, 154301 (2012)
4. M. Baba, Y.-C. Hsu, S. H. Lin, et al., **J. Chem. Phys.** *131*, 224318 (2009)

5. Y.Kowaka, M. Baba, T, Ishimoto, et al., **J. Mol. Spectrosc.** *260*, 72 (2010)
6. M. Baba, **J. Phys. Chem. A** *115*, 9514 (2011)

B2

Comb-referenced spectroscopy of aromatic hydrocarbons

M. Misono, A. Nishiyama, M. Baba
Fukuoka Univ., Univ. of Electro-Communications, Kyoto Univ.
e-mail: m-misono@fukuoka-u.ac.jp

Polyatomic molecules show interesting dynamics in their electronic excited states. We have been studied the dynamics by high-resolution spectroscopy with a supersonic molecular beam or by Doppler-free two-photon absorption spectroscopy. We have already observed and analyzed high-resolution spectra of small aromatic hydrocarbons, such as benzene[1] and naphthalene[2,3]. Recently, we have developed our measurement system to observe spectra of larger aromatic hydrocarbons, such as, coronene, perylene, and 1,2-benzanthracene. To observe high-resolution spectra of these molecules, we expand the wavelength range of our system.

Our system is composed of two parts: high-resolution spectroscopic system and precision frequency measurement system. The light source for high-resolution spectroscopy is a single mode Ti:Sapphire laser (Coherent, 899-29). Most of the output of the light source is input into a second harmonics generator (Spectra-Physics, Wavetrain SC) to generate second harmonics. The second harmonic wave passes across a supersonic molecular beam in a vacuum chamber. The precision frequency measurement system is equipped with an Er fiber comb or a Ti:Sapphire comb. We use one of the combs according to their characteristics. The Er fiber comb is so stable that it operates without tuning whole day, and its wavelength range is restricted to 1480 - 1660 nm and 740 nm - 830 nm. On the other hand, the wavelength range of the Ti:Sapphire comb is ranged 500 - 1200 nm, however, it needs frequent tuning every few hours. A part of the single mode Ti:Sapphire laser output is split and overlapped with the comb output to observe the beat frequency.

In the talk, we will explain the detail of our system, and will introduce some results of spectroscopy of aromatic hydrocarbons.

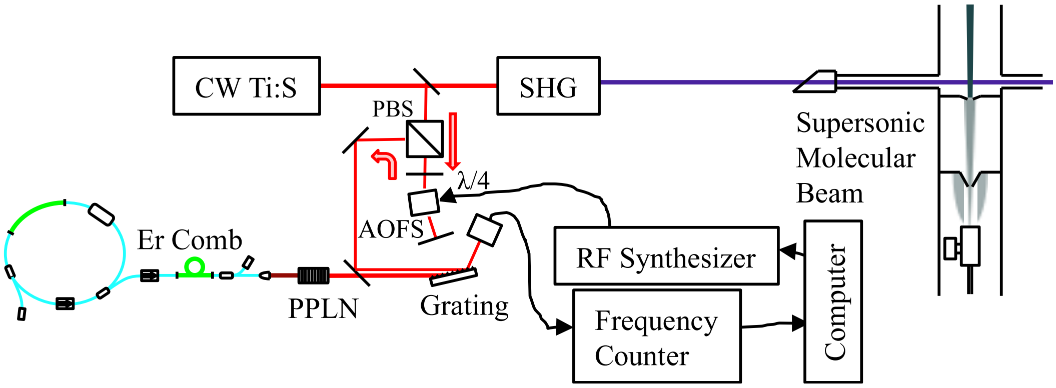

References

1. M. Misono, J. G. Wang, M. Ushino, M. Okubo, H. Katô, M. Baba, and S. Nagakura, J. Chem. Phys., 116, 162-171 (2002).
2. A. Nishiyama, K. Nakashima, A. Matsuba, and M. Misono, J. Mol. Spectrosc., 318, 40-45 (2015).
3. K. Yoshida, Y. Semba, S. Kasahara, T. Yamanaka, and M. Baba, J. Chem. Phys., 130, 194304 (2009).

B3

Infrared spectra of protonated and hydrogenated corannulene ($C_{20}H_{10}$) using matrix isolation in solid *para*-Hydrogen

<u>Pavithraa Sundararajan</u>[1], Masashi Tsuge[2], Yuan-Pern Lee[1,3]

[1] Dept. Applied Chemistry, NCTU, Hsinchu 30010, Taiwan
[2] Institute of Low Temperature Science, Hokkaido University, Japan.
[3] Institute of Molecular Siences, Academia Sinica, Taipei 10617.
E-mail: pavi.nctu@gmail.com

Polycyclic aromatic hydrocarbons (PAH) are of significant importance in both terrestrial and extra-terrestrial environments. PAH gained attention in the interstellar chemistry as they are attributed to be the emitters of the Unidentified IR (UIR) emission bands. However, till date, no single PAH could be positively assigned to the UIR.

Corannulene ($C_{20}H_{10}$) is a fragment of Bucky ball C_{60} and has a bowl-like structure. It was proposed to be an intermediate in the formation of fullerenes in outer space [1]. Since proton sources such as H^+ and H_3^+ are abundant in Interstellar Medium (ISM), the proton transfer reactions to produce protonated species are likely to occur. Because the proton affinities of PAH are high, protonated PAH are postulated to be present in the ISM [2]. Protonated corannulene ($H^+C_{20}H_{10}$) hence could be of astrophysical significance and hence it is imperative to investigate the infrared features of $H^+C_{20}H_{10}$ in the laboratory.

Our recent technique of using electron bombardment on a p-H_2 matrix to produce protonated/hydrogenated species cleanly and efficiently can provide direct IR absorption spectrum covering a wide range [3]. The experiments were carried out with a closed-cycle helium refrigerator, capable of cooling to 3.3 K, which was coupled with a FTIR having an HgCdTe detector to cover the spectral range 500-4000 cm^{-1}. Protonated corannulene ($H^+C_{20}H_{10}$) and their neutral counterparts were produced upon electron bombardment of the matrix during deposition of $C_{20}H_{10}$ mixed in p-H_2 over a period of 10 hours [4]. The matrix was then maintained in darkness for 30 hours followed by secondary photolysis using light at various wavelengths from several light-emitting diodes. The protonated species became diminished after maintaining the matrix in darkness, whereas its neutral counterparts were produced. Infrared absorption features, grouped according to the behavior after maintaining the matrix in darkness and upon secondary photolysis were assigned to several conformers of protonated (or hydrogenated) isomers of $C_{20}H_{10}$ by comparison with the quantum-chemically calculated IR spectra. Two protonated species of $C_{20}H_{10}$ (with proton at the *hub and rim* sites) and their respective neutral counterparts are unambiguously identified.

References .

1. Rouillé, G., C. Jäger, et al. **ChemPhysChem** *9(14): 2085-2091* (2008).

2. Pathak, A. and P. J. Sarre. **Monthly Notices of the Royal Astronomical Society: Letters** *391(1): L10-L14* (2008).
3. Wu, Y.-J., X. Yang, et al. **The Journal of Chemical Physics** *120(3): 1168-1171* (2004).
4. Tsuge, M., C.-Y. Tseng, et al**. Physical Chemistry Chemical Physics** (2018).

B4

Supersonic-jet laser spectroscopy of nonplanar aromatic hydrocarbon

Ayumi Kanaoka[1], Masaaki Baba[1], Masashi Tsuge[2,3] and Yuan-Pern Lee[2]
1, Kyoto University, Japan
2, National Chiao Tung University, Taiwan
3, Hokkaido University, Japan
kanaoka.ayumi.55u@st.kyoto-u.ac.jp

Buckybowl (sumanene and corannulene) and FLAP (FLexible Aromatic Photo-responsive molecule) have interest features and they are all nonplanar. We observed their fluorescence spectra and dispersed spectra in a supersonic-jet. By comparing with the results of theoretical calculation, we provided the approximate geometrical structure of the isolated molecule and exciting energy, respectively. We gained excitation energy in very good agreement with those obtained by ab initio theoretical calculation (TD-DFT(B3LYP)/6-31G(d,p) or SAC-CI/6-31G).

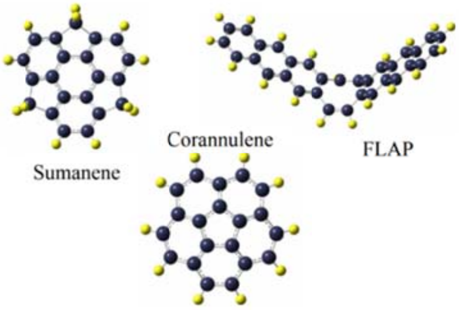

Buckybowls are parts of fullerene and have bowl shaped π systems. In terms of vibrations both are resemble. But they have some differences. For example, the $S_1\,{}^1A_1 \leftarrow S_0\,{}^1A_1$ transition is symmetry allowed for sumanene[1], whereas the $S_1\,{}^1E_2 \leftarrow S_0\,{}^1A_1$ is forbidden for corannulene.

FLAP consists of two anthracenes and one cyclooctatetraene and its structure is V-shaped. Some of its vibrational modes resembles that of anthracene[2]. It emits blue fluorescence in gas phase. However, that in solution emits strong green fluorescence.[3] Because of Franck-Condon principle, FLAP whose structure changes dramatically in the excited state is hard to relax to V-shaped one. We suppose that green fluorescence results from an isomer of FLAP. Isomerization occurs more easily in solution by interacting with solvent than in gas phase.

LIF Spectra of Corannulene

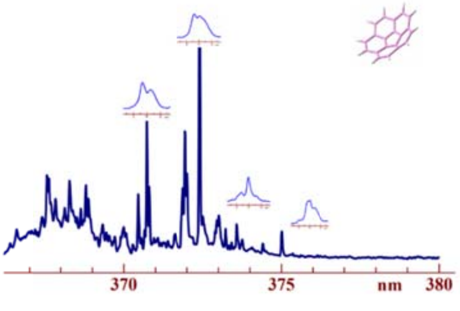

References

1. S. Kunishige, M. Kawabata, M. Baba, et al., **J. Chem. Phys.** *139*, 044313 (2013).
2. M. Baba, M. Saitoh, K. Taguma, et al., **J. Chem. Phys.** *130*, 134315 (2009).
3. C. Yuan, S. Saito, C. Camacho, et al., **J. Am. Chem. Soc.** *135*, 8842-8845 (2013).

B5

Infrared spectrum of proton-bound nitrogen dimer N_2–H^+–N_2 in solid *para*-H_2

Masashi Tsuge,[1,2] **Hsin-Yi Liao,**[3] **Jake A. Tan,**[4] **Jer-Lai Kuo,**[4] **and Yuan-Pern Lee**[1,4]
[1]Department of Applied Chemistry and Institute of Molecular Science,
National Chiao Tung University
[2]Institute of Low Temperature Science, Hokkaido University
[3]Department of Science Education, National Taipei University of Education
[4]Institute of Atomic and Molecular Sciences, Academia Sinica
e-mail: tsuge@lowtem.hokudai.ac.jp

The existence of proton-bound dimers such as N_2–H^+–N_2 in the interstellar medium has been proposed.[1] Proton-bound dimers, represented as X–H^+–Y, are also important subject in spectroscopy because these species are regarded as an intermediate in the proton-transfer reaction $XH^+ + Y \rightarrow [X\text{–}H^+\text{–}Y] \rightarrow X + HY^+$; the strong anharmonicity associated with the proton motion of these species makes an understanding their spectra challenging.

In this work, the proton-bound nitrogen dimer, N_2–H^+–N_2 and its isotopologues were investigated by infrared spectroscopy.[2] These species were produced on electron-bombardment of mixtures of N_2 (or $^{15}N_2$) and *para*-hydrogen or *normal*-D_2 during deposition at 3.2 K. Reduced-dimension anharmonic vibrational Schrödinger equations were constructed to account for the strong anharmonic effects in these species. Fundamental lines of proton motions in N_2–H^+–N_2 were observed at 715.0 (NH^+N antisymmetric stretch, ν_4), 1129.6 (NH^+N bend, ν_6), and 2352.7 (antisymmetric NN/NN stretch, ν_3) cm^{-1}, in agreement with values 763, 1144, and 2423 cm^{-1} predicted with anharmonic calculations using the discrete-variable representation method at the CCSD/aug-cc-pVDZ level of theory. Lines at 1030.2 and 1395.5 cm^{-1} were assigned to combination bands involving $n\nu_2 + \nu_4$ (n = 1 and 2) according to theoretical calculations; ν_2 is the $N_2 \ldots N_2$ stretching mode.

If time permits, we will present results on proton-bound dimers formed between N_2 and CO; i.e., N_2–H^+–CO and/or N_2–H^+–OC.

References

1. Q. Yu, J. M. Bowman, R. C. Fortenberry *et al.*, **J. Phys. Chem. A**, *119*, 11623-11631 (2015).
2. H.-Y. Liao, M. Tsuge, J. A. Tan, J.-L. Kuo, and Y.-P. Lee, **Phys. Chem. Chem. Phys.**, *19*, 20484-20492 (2017).

B6

Analysis of infrared absorption spectra of solid methanol at low temperature after hydrogen atom bombardment

Yukiko Yarnall [1, 2], **Hiroshi Hidaka**[1], **Yasuhiro Oba** [1], **Masashi Tsuge** [1], **Tetsuya Hama** [1], **Akira Kouchi** [1], **Naoki Watanabe** [1]
[1]Institute of Low Temperature Science, Hokkaido University, Sapporo, Hokkaido, Japan.
[2]Chemistry and Biochemistry, George Mason University, Fairfax, VA, United States.
yyarnall@masonlive.gmu.edu, hidaka@lowtem.hokudai.ac.jp, watanabe@lowtem.hokudai.ac.jp

Methanol (CH_3OH) is one of the important molecules in the field of astrochemistry, because it is abundant in interstellar medium (ISM) and also can be a precursor of prebiotic molecules. Therefore, many research groups have studied its formation process theoretically and experimentally. Formation process of CH_3OH is now well understood as the successive CO hydrogenation via H_2CO formation by quantum tunneling reaction on interstellar grain surfaces[2]. Recently, the destruction of CH_3OH by backward reactions such as $CH_3OH \rightarrow H_2CO$ by H abstraction reactions were observed at co-deposition of CH_3OH and H atoms by Chuang et al. (2016)[1]. In the present study, we conducted experiments of the H abstraction reaction of CH_3OH by H atoms exposure on two different ices, pure solid CH_3OH and amorphous solid water as more realistic ice grain analogues. We will discuss the phenomena including backward reaction which are triggered by H atoms exposure of CH_3OH.

References

1. K.-J. Chuang, G. Fedoseev, S. Ioppolo, E.F. van Dishoeck and H. Linnartz. **Monthly Notices of the Royal Astronomical Society**,*455*,1702-1712 (2016).
2. N. Watanabe and A Kouchi. **The Astrophysical Journal,***571*, L173–L176 (2002).

B7

Hydrogen abstraction from methyl formate by H-atom: Infrared absorption spectra of •$C(O)OCH_3$ radical isolated in solid *para*-hydrogen

Karolina A. Haupa[a)] **and Yuan-Pern Lee**[a), b)]

[a)] Department of Applied Chemistry and Institute of Molecular Science, National Chiao Tung
University, Hsinchu 30010, Taiwan;
[b)] Institute of Atomic and Molecular Sciences, Academia Sinica, Taipei 10617, Taiwan
e-mail: karolina.haupa@gmail.com

The systematic astronomical observations lead to identification of more than 250 molecules in interstellar medium (ISM).[1] Since its discovery in 1975, methyl formate (MF, $HC(O)OCH_3$) was observed in significant amount in varied astrophysical environments including hot cores, protoplanetary nebula, and comets. The formation of methyl formate in CO/ CH_3OH ices exposed to H atoms and/or UV irradiation at 14 K was reported by Chuang *et al.*[2] However, according to the reported H-atom exposure and UV irradiation efficiency, the amount of $HC(O)OCH_3$ predicted is much smaller than astronomical observations. The possibility of secondary reactions of $HC(O)OCH_3$ under the H-atom exposed environments should be considered.

We investigated the reaction H + $HC(O)OCH_3$ in solid *para*-hydrogen (*p*-H_2) at 3.3 K with infrared absorption spectra. Cl_2 molecules (co-deposited with $HC(O)OCH_3$) in *p*-H_2 was irradiated at 365 nm to produce Cl atoms that reacted, upon IR irradiation of the *p*-H_2 matrix, readily with nearby H_2 to produce mobile H atoms. We found that hydrogen abstraction of the carbonyl hydrogen of $HC(O)OCH_3$ is a dominant process. New lines at 3049.1 (ν_1), 3019.6 (ν_{11}), 2945.3 (ν_2), 1785.2 (ν_3), 1442.7 (ν_{12}), 1409.3 (ν_5), 1170.6 (ν_6), 1104.6 (ν_7), and 880.5/879.4 cm^{-1} (ν_8) are assigned to the methoxycarbonyl, •$C(O)OCH_3$, radical. The weak features at 1152.9 (ν_8) and 996.3/994.4 cm^{-1} (ν_{12}) are tentatively assigned to the formyloxymethyl, $HC(O)OCH_2$•, radical. These assignments were derived according to the consideration of possible reactions and comparison of observed vibrational wavenumbers and their IR intensities with values predicted quantum-chemically with the B3LYP/aug-cc-pVTZ method. Methyl formate can react with H atom at 3.3 K. The abstraction of the carbonyl hydrogen is a dominant channel in the H + $HC(O)OCH_3$ reaction and the branching ratio for formation of $(O)OCH_3$ and HC(O)The role of H + $HC(O)OCH_3$ reaction in previous laboratory experiments and reaction mechanism of $HC(O)OCH_3$ in ISM is discussed.

References

1. https://www.astro.uni-koeln.de/cdms/molecules
2. K. –J. Chuang, G. Fedoseev, D. Qasim, S. Ioppolo, E. F. van Dishoeck, and H. Linnartz, **Mon. Not. R. Astr. Soc.**, *467*, 2552 (2017).

B8

2C-R4WM Spectroscopy of the NO_3 $\tilde{B}\ {}^2E' - \tilde{X}\ {}^2A_2'$ system

Masaru Fukushima and Takashi Ishiwata
Faculty of Information Sciences, Hiroshima City University, Asa-Minami, Hiroshima 731-3194,
Japan. e-mail: fukushim@info.hiroshima-cu.ac.jp

We have generated NO_3 in supersonic free jet expansions, and observed the laser induced fluorescence (LIF) and two-color resonant four-wave mixing (2C-R4WM) signals of the $\tilde{B}\ {}^2E' - \tilde{X}\ {}^2A_2'$ electronic transition. We have measured dispersed fluorescence (DF) spectra from the single vibronic levels. Vibrational structure of the DF spectrum from the vibration-less level is categorized into three parts. Region II: The structure in the region below 1850 cm^{-1}, except the ν_1 and ν_3 fundamental regions (Region I), ~ 1050 and 1500 cm^{-1}, respectively, is understandable as the ν_4 progressions, 4^0_n and $1^0_1 4^0_n$. Region III: The structure above 1850 cm^{-1} is too complicated to interpret the structure. Region I: The ν_1 and ν_3 regions are now active for discussion, and thus we have tried to measure the rotationally resolved 2C-R4WM spectra. The observation of the 2C-R4WM signals has been restricted those through J' = 0.5 of the $\tilde{B}\ {}^2E'_{3/2}$ state only, as reported previously [1], the reason of which has been unsolved yet. The 2C-R4WM spectrum of the 1500 cm^{-1} region shows the K = 0 and N = 1 level of an a_1' level remarkably (which may be attributed to the $2\nu_2$ or $4\nu_4$ level, or mix of them, but has not been concluded yet), and the 4WM transition energy observed agrees with that derived from IR hot-band analysis [2]. On our higher resolution measurement of the DF spectrum, it has been found that there is an additional level near the ν_1 fundamental [3], and accordingly the 2C-R4WM spectrum of the ν_1 region also has the corresponding two bands. The K = 0 and N = 1 level of the ν_1 fundamental has been identified for the first time. The other, additional band consists of two rotational transitions separated by 0.27 cm^{-1}. Although the 0.27 cm^{-1} separation is about 10 times larger than the spin splitting, ~0.025 cm^{-1}, of the K = 0 and N = 1 levels at the other a_1' levels with l = 0, such as vibration-less and ν_1 (the latter value of which, 0.025 cm^{-1}, cannot be resolved under our instrumental resolution), the two transitions are thought to correspond to those terminated to two spin sub-levels, J = 0.5 and = 1.5, at the present. On our interpretation on $3\nu_4$, electronic angular momentum, Λ_i, induced by the vibrational angular momentum, l, generates the large splitting, ~160 cm^{-1}, between the a_1' and a_2' levels of $3\nu_4$, and this additional a_1' level is assigned to $3\nu_4$ with $l = \pm 3$ [3,4]. For Σ vibronic levels with K = 0, such as v_d = 1 and l = 1, of a ${}^2\Pi$ electronic state, it is well known that ${}^2\Sigma^{(+)}$ and ${}^2\Sigma^{(-)}$ vibronic levels have relatively large Ω- or ρ-type doubling due to non-zero Λ, in spite of the Σ vibronic levels [5]. It is thought that the unexpectedly large spin splitting, 0.27 cm^{-1}, between the J = 0.5 and = 1.5 levels at $3\nu_4$ with $l = \pm 3$ is induced by spin-vibration interaction, which has been discussed for degenerate vibronic levels of non-degenerate electronic states, ${}^2\Sigma$ and ${}^3\Sigma$, of linear polyatomic molecules [6].

1. M. Fukushima and T. Ishiwata, **71st ISMS**, *paper RF01* (2016).
2. K. Kawaguchi *et al.*, **J. Mol. Spectrosco.** *268*, 85 (2011).
3. M. Fukushima and T. Ishiwata, **68th ISMS.**, *paper WJ03* (2013).
4. E. Hirota, **J. Mol. Spectrosco.** *343*, 81 (2018).
5. J. Hougen, **J. Chem. Phys.** *36*, 519 (1964).
6. A. J. Merer and J. M. Allegretti, **Can. J. Phys.** *49*, 2859 (1971).

B9

Rotational Investigation on the Conformational Preferences and Reactivity of Criegee Intermediates

Carlos Cabezas,[a] **Jean-Claude Guillemin**[b] **and Yasuki Endo**[a]
[a]National Chiao Tung University, [b]Institut des Sciences Chimiques de Rennes
ccabezas@nctu.edu.tw, jean-claude.guillemin@ensc-rennes.fr, endo@nctu.edu.tw

The Criegee intermediates, R_1R_2COO (CI's), are produced by the ozonolysis reaction, the reaction of unsaturated hydrocarbons with ozone[1]. The produced CI's have large excess energy, and undergo unimolecular decay producing the OH radical. They are thus considered to be important sources of the OH radical in atmospheric chemistry. On the other hand, they react quickly with many trace atmospheric gases, such as SO_x, NO_x, and water, when they are stabilized. Since the first direct detection of the simplest CI, CH_2OO[2], studies of CI's are performed very extensively in recent years, where reactivities of various alkyl substituted CI's and conformer specific reactivities have been discussed. In our laboratory, we are studying various CI's and their reaction products by Fourier-transform microwave spectroscopy in the cm wave region. Owing to very high resolution and sensitivity, it is possible to study various alkyl substituted CI's identifying all the possible isomers and conformers, which are of fundamental importance in understanding reactions of CI's in atmospheric chemistry. In this talk, I will present results obtained during last two years.

Since the first detection of the simplest CI, CH_2OO [3] together with the methyl derivatives (R_1, R_2=H, CH_3) [4-6] by microwave spectroscopy, we have started systematic studies of larger alkyl substituted CI's. So far, CI's with R_1, R_2= CH_3, C_2H_5, C_3H_7 have been observed, where various conformers for each species have been identified. Barrier heights of methyl tops for those containing methyl groups have been determined. Differences of the barrier heights are discussed in relation to the molecular structures.

In relation to the reactions of stabilized CI's with atmospheric trace gases, pre-reaction complex of CH_3CHOO with water has been detected in addition to their reaction products, hydroxyethylhydroperoxide (HEHP) [7]. The reaction product of CH_2OO with HCl, chloromethylhydroperoxide (CMHP) was also detected [8]. However, no pre-reaction complex has been detected for this system.

References

[1] R. Criegee, **Angew Chem. Inter. ed. Engl.** *14,* 745 (1975).

[2] C. A. Taatjes, G. Meloni, T. M. Selby, A. J. Trevitt, D. L. Osborn, C. J. Percival, D. E. Shallcross, **J. Am. Chem. Soc.** *130*, 11883 (2008).

[3;4;5;6] M. Nakajima and Y. Endo, **J. Chem. Phys.** *139*, 10113 (2013); *140*, 134302 (2014); *143*, 164307 (2015); *145*, 244307 (2016).

[7] C. Cabezas and Y. Endo, **J. Chem. Phys.** *148*, 014308 (2018)

[8] C. Cabezas and Y. Endo, **ChemPhysChem**, *18*, 1860 (2017).

B10

High resolution spectroscopy and reaction kinetics of simplest Criegee intermediates studied by mid-IR laser spectrometer

Y.-P. Chang, A. J. Merer, H.-H. Chang, L.-J. Jhang, W. Chao and J. J.-M. Lin
Department of Chemistry, National Sun Yat-sen University, Kaohsiung, Taiwan, R.O.C
e-mail: ypchang@mail.nsysu.edu.tw

Criegee intermediates (CIs) are highly reactive carbonyl oxides created during the ozonolysis of alkenes. Many recent studies have unveiled the important roles of CIs in atmospheric chemistry. Furthermore, CI chemistry highly depends on structure, such as substitution groups and conformations[1]. Recently, Y.-P. Lee et al.[2,3] demonstrated the infrared detection of prototypical CIs using a step-scan Fourier-transform spectrometer. Inspired by their works, we built up a transient absorption spectrometer utilizing a mid-infrared quantum cascade laser, allowing for resolving ro-vibrational spectra of CIs. As a proof of principle study, we have measured the transient absorption spectra of gas phase CH_2OO in the region of 1273 cm^{-1} to 1290 cm^{-1} with a resolution better than 0.004 cm^{-1}.[4] Analysis of the absorption spectrum has provided precise values for the vibrational frequency and the rotational constants, with fitting errors of a few MHz. The determined ratios of the rotational constants, $A'/A'' = 0.9986$, $B'/B'' = 0.9974$ and $C'/C'' = 1.0010$, and the relative intensities of the a- and b-type transitions, 90:10, have a good agreement with literature values from a latest high-level *ab initio* calculation. We also observed the rotational perturbations by other vibrational modes which disrupt the structure for $K = 4$ and $K \geq 6$. We also studied the kinetics of CH_2OO reaction with ozone via monitoring CH_2OO with this transient absorption spectrometer, which utilized fast chirped IR pulse train from the QCL.[5] The measured rate coefficient at 298 K and 30 Torr is $(6.7\pm0.5)\times10^{-14}$ cm^3sec^{-1}, independent of pressure from 30 to 100 Torr. The result indicates that previous *ab initio* calculations either underestimated or overestimated this reaction rate by one order of magnitude or more. The result also implies that in laboratory studies of ozonolysis of alkenes, the reaction of CIs with ozone may play a role. However, this reaction would not compete with other CH_2OO sinks in the atmosphere.

References

1. J. J.-M. Lin and W. Chao, **Chem. Soc. Rev.**, (2017). DOI: 10.1039/c7cs00336f
2. Y.-T. Su, Y.-H. Huang, H. Witek and Y.-P. Lee, **Science**, *340*, 174 (2013).
3. H.-Y. Lin, Y.-H. Huang, X. Wang, J. M. Bowman, Y. Nishimura, H. Witek and Y.-P. Lee**, Nat. Commun.**, *6*, 7012 (2015).
4. Y.-P. Chang, A. J. Merer, H.-H. Chang, L.-J. Jhang, W. Chao and J. J.-M. Lin, **J. Chem. Phys.**, *146*, 244302 (2017).
5. Y.-P. Chang, H.-H. Chang, and J. J.-M. Lin, **Phys. Chem. Chem. Phys.**, *20*, 97 (2018).

B11

High-resolution spectra of the simplest Criegee intermediate CH_2OO between 880 and 932 cm^{-1}

Pei-Ling Luo[1], **Yasuki Endo**[1], **and Yuan-Pern Lee**[1,2]
[1]Department of Applied Chemistry and Institute of Molecular Science, National Chiao Tung University, Hsinchu 30010, Taiwan
[2]Institute of Atomic and Molecular Sciences, Academia Sinica, Taipei 10617, Taiwan
e-mail: kkmion@gmail.com

The Criegee intermediates (CI) play critical roles in atmospheric chemistry. CH_2OO is the simplest CI and its characterization is important for investigations of reaction mechanisms and molecular structure. Spectral detections of CH_2OO have been reported with various methods, such as VUV photoionization mass spectrometry[1], microwave spectroscopy[2], UV absorption[3], IR absorptions[4,5] and THz spectrometry[6].

In this work, the high-resolution spectra of the OO-stretching (ν_6) band of CH_2OO in the range of 10.73-11.36 μm (932-880 cm^{-1}) have been demonstrated using a cw quantum cascade laser (QCL) system coupled with a multi-pass Herriott absorption cell. The CH_2OO was produced from the reaction of $CH_2I + O_2$ in a flowing mixture of CH_2I_2/O_2 (1/213) at 298K and 3.2 Torr upon irradiation at 248 nm with an excimer laser. The spectra were recorded by step-scanning the frequency of QCL with a step size of ~0.0016 cm^{-1} and calibrated using a C_2H_4 reference cell and a germanium etalon. Over one thousand lines were assigned and used for fitting of molecular constants of CH_2OO. The rotational constants (A', B', and C') with ~0.1 MHz uncertainties and the high-order parameters (Δ_J, Δ_{JK}, Δ_K, δ_J, and δ_K) were determined and compared with theoretical predictions. Furthermore, we observed the rotational perturbations of $K_a = 3$, $K_a = 6$, and $K_a \geq 11$ on the high J levels. In particular, for $K_a = 6$, the plot of the frequency shifts on J' shows an avoided-crossing which can be analyzed with rotational energies of ν_6 and ν_8 modes of CH_2OO.

References

1. O.Welz, J. D. Savee, D. L. Osborn, S. S.Vasu, C. J. Percival, D. E. Shallcross, and C. A. Taatjes, Science **335**, 204 (2012).
2. M. Nakajima, Q. Yue, J. Li, H. Guo, and Y. Endo, Chem. Phys. Lett. **621**, 129 (2015).
3. W.-L. Ting,Y.-H. Chen,W. Chao, M. C. Smith, and J. J.-M. Lin, Phys. Chem. Chem. Phys. **16**, 10438 (2014).
4. Y.-T. Su, Y.-H. Huang, H. A.Witek, and Y.-P. Lee, Science **340**, 174 (2013).
5. Y.-H. Huang, J. Li, H. Guo, and Y.-P. Lee, J. Chem. Phys. **142**, 214301 (2015).
6. A. M. Daly, B. J. Drouin, and S. Yu, J. Mol. Spectrosc. **297**, 16 (2014).

B12

Reaction of the Criegee Intermediate CH_2OO with HCl Investigated with a Step-scan Fourier-transform Spectrometer

Wei-Che Liang[1], **Yuan-Pern Lee**[1,2]
[1]Department of Applied Chemistry and Institute of Molecular Science, National Chiao Tung University, 1001, Ta-Hsueh Road, Hsinchu 30010,Taiwan
[2]Institute of Atomic and Molecular Sciences, Academia Sinica, Taipei 10617, Taiwan
yplee@mail.nctu.edu.tw

The Criegee intermediates, which are carbonyl oxides produced in ozonolysis of unsaturated hydrocarbons,[1] play important roles in the production of OH, aerosols and organic acids in the atmosphere. Criegee intermediates react readily with other atmospheric species such as NO_2, SO_2, $(H_2O)_2$ and HCl. The reaction of CH_2OO with HCl was reported to be rapid, with a rate coefficient of 4.6×10^{-11} cm^3 $molecule^{-1}$ s^{-1}.[2] Quantum-chemical calculations indicate that the reaction CH_2OO + HCl proceeds through a barrierless association reaction to form chloromethyl hydroperoxide (CMHP, CH_2ClOOH), which was predicted to have two stable conformation, denoted as *gauche*-CMHP and *anti*-CMHP; both conformers were observed by microwave spectroscopy.[3]

In this work, a step-scan Fourier-transform spectrometer coupled with a multipass absorption cell was employed to record temporally resolved infrared (IR) absorption spectra of the reactants and products during the reaction of CH_2OO with HCl in a flow system. CH_2OO was produced from the reaction of O_2 with CH_2I, which was produced via photolysis of CH_2I_2 at 308 nm.[4] Time-resolved IR absorption spectra were recorded at resolution 0.25 cm^{-1}. Observed bands at 819.0, 889.7, 1061.3, 1310.2 and 1359.7 cm^{-1} are assigned to CMHP. The observed wavenumbers and relative intensities agree with the anharmonic vibrational wavenumbers and IR intensities predicted with the B3LYP/aug-cc-pVTZ method. Further investigations on the rotational contour are in progress in order to unravel the contributions of each conformer.

References

1. R. Criegee and G. Wenner, **J. Liebigs Ann. Chem.** *564*, 9 (1949).
2. E. S. Foreman et al., **Angew. Chem. Int. Ed.** *55*, 1 (2016).
3. C. Cabezas and Y. Endo, **ChemPhysChem**. *18*, 1860 (2017).
4. Wang, Chung, and Lee, **J. Chem. Phys.** *145*, 154303 (2016)

B13

Theoretical calculation of UV spectrum for Criegee intermediates

Cangtao Yin, **Kaito Takahashi**
Institute of Atomic and Molecular Sciences, Academia Sinica
ctyin1986@gmail.com

Criegee intermediates (CIs) may play important roles in atmospheric chemistry, and quantify their absolute UV cross section could be a way of clarifying the significantly different reactivity of CIs. However, few experimental measurements have been reported, and their results differ a lot. In theory, we only found three studies in the literature[1-3] that have calculated the UV spectrum of the simplest CI, CH_2OO. To the best of our knowledge, no studies have considered substituted CIs. By studying all the CIs with up to three carbon atoms, CH_2OO, CH_3CHOO, $(CH_3)_2COO$, CH_3CH_2CHOO, $CH_2CHCHOO$, CHCCHOO, we intend to obtain understanding on the substitution effect. First we performed large active space DW-CASSCF calculation followed by MRCI calculations with a smaller active space. We found that big active space is essential when performing CASSSCF calculation while using MRCI with Davidson's correction using aug-cc-pVTZ basis with (8o, 8e) active space is good enough to give a reasonable result. Our results for CH_2OO, *syn*-CH_3CHOO, *anti*-CH_3CHOO and $(CH_3)_2COO$ agree well with experimental values[4-6]. For the unsaturated CIs, which we have very limited experimental data, we obtained distinct conformer specific UV spectra, which may help the future detection of these CIs. Lastly, we showed that for all the CIs considered in this work, the photolysis rate only varied between 0.05 to 0.6 sec^{-1}. These rates are too slow to compete with other atmospheric decay pathways such as CI thermal decomposition and reaction with water or SO_2.

References

1. Q. Meng, H.-D. Meyer, **J. Chem. Phys.**, *141*, 124309 (2014).
2. K. Samanta, J. M. Beames, M. I. Lester, J. E. Subotnik, **J. Chem. Phys.**, *141*, 134303 (2014).
3. R. Dawes, B. Jiang, H. Guo, **J. Am. Chem. Soc.**, *137*, 50-53 (2015).
4. W.-L. Ting, Y.-H. Chen, W. Chao, M. C. Smith, J. J.-M. Lin, **Phys. Chem. Chem. Phys.**, *16*, 10438-10443 (2014).
5. M. C. Smith, W.-L. Ting, C.-H. Chang, K. Takahashi, K. A. Boering, J. J.-M. Lin, **J. Chem. Phys.**, *141*, 074302 (2014).
6. Y.-P. Chang, C.-H. Chang, K. Takahashi, J. J.-M. Lin, **Chem. Phys. Lett.**, *653*, 155-160 (2016).

B14

Photothermal interferometric gas sensing in hollow-core optical fibers

Chenyu Yao and Wei Ren
Department of Mechanical and Automation Engineering, The Chinese University of Hong Kong,
New Territories, Hong Kong
e-mail: renwei@mae.cuhk.edu.hk

Photothermal interferometry (PTI) is a highly sensitive and selective technique that measures material properties based on the heating generated by optical absorption of the material. In gas sensing, the wavelength dependent optical absorption induces a change of the reflective index that causes a phase shift of light passing through the heated region. The photothermal signal is proportional to the absorption coefficient, the absorption length, and the optical intensity of the pump light. Therefore, the detection sensitivity of PTI can be significantly improved by confining the laser beams in a tiny hollow-core fiber (HCF). The mid-infrared domain offers opportunities for more sensitive gas sensing as many molecules have their fundamental absorption bands in this spectral region. Typical mid-infrared HCFs include the inner-surface-coated HCF with a relatively large core diameter and high bending loss. A novel HCF, node-less anti-resonant fiber, has recently demonstrated a smaller core diameter, lower bending loss, and higher transmission in the mid-infrared. In this presentation, we report the demonstration of the PTI for trace gas sensing in mid-infrared hollow-core fibers.

References

1. W. Jin, Y. Cao, F. Yang and H. L. Ho, **Ultra-sensitive all-fibre photothermal spectroscopy with large dynamic range**, *Nature Communications* 6 (2015).
2. Z. Li, Z. Wang, F. Yang, W. Jin, and W. Ren, **Mid-infrared fiber-optic photothermal interferometry**, *Optics Letters*, 42 (2017): 3718-3721.

B15

Direct frequency comb spectroscopy and Its Application

Tze-Wei Liu
Institute of Atomic and Molecular Science, Academia Sinica, Taiwan
Physical Department, National Central University, Taiwan
e-mail: b91202001@gmail.com

We report the direct frequency comb spectroscopy of $6S_{1/2}$ to $8S_{1/2}$ transition in ^{133}Cs vapor. That is, the stepwise excitation through the $6P_{3/2}$ intermediate state is performed directly with a broadband-femtosecond laser pulse. The counter-propagating laser beam is focused into a 68℃ Cs vapor cell. The repetition rate of the frequency comb is scanned and we detect the blue fluorescence from the $7P_{1/2,\ 3/2}$ to $6S_{1/2}$ decay. In fact, there are multi decay channels emit this blue fluorescence, such as from 8S, 9S, or 7D states to 6S state. And there is a spatial light modulator in the laser beam paths in order to isolate the excitations to the different states except $6S_{1/2}$ to $8S_{1/2}$.

It is surprised to us that the resonant-enhanced two-photon transition has a spectral width of only 1.23 MHz (FWHM), comparable to that obtained by direct two-photon Doppler-free spectroscopy of a CW laser at 822 nm [1]. Note that the 5 MHz linewidth of the intermediate states does not contribute to the aforementioned linewidth resolved by comb laser directly, which enables us to utilize it for comb laser stabilization and the result will present in conference.

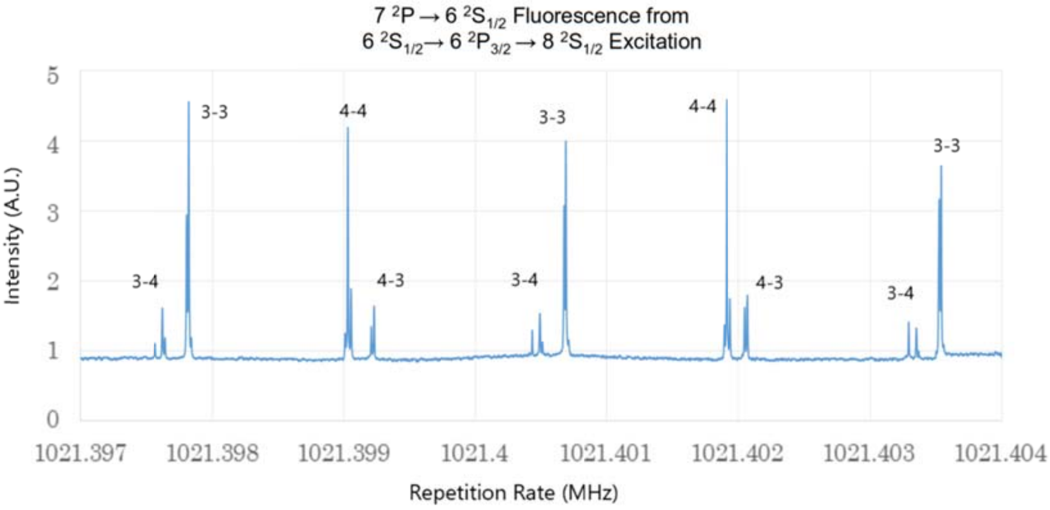

References

1. Chien-Ming Wu, Tze-Wei Liu, Ming-Hsuan Wu, Ray-Kung Lee and Wang-Yau Cheng, "Absolute frequency of cesium 6S-8S 822-nm two-photon transition by a high-resolution scheme", *Opt. Lett.* 38, 16, 3186 (2013)

B16

Narrow-bandwidth Coherent-Population-Trapping Resonance under Polarization Modulation

Bo-Wei Chen

Laboratory of Comb Laser Based Spectroscopy, Department of Physics, National Central University, Taiwan

e-mail: paulxxxtw@gmail.com

We introduce a convenient scheme that enhances the performance of coherence population trap (CPT), and that leads us to improve the signal/noise ratio on a 1 kHz-linewidth resonance in the buffer gas cesium cell. In this scheme, the polarization of a bichromatic laser beam is modulated between linear and circular polarization by an electro-optic modulator. The advantage of applying this technique is two-fold: One is to keep away optical pumping to extreme Zeeman sublevel for avoiding the reduction of transition amplitude; another is to chop the CPT for lock-in amplifier since we have observed that would show different contrasts with the light between linear and circular polarization. Thus, we can apply this interesting feature to remove the Doppler background and improve signal-to-noise ratio.

Moreover, we also study the behavior of a three-level system with sinusoidal polarization-modulated light. Surprisingly, as the modulation frequency exceeds the dephasing rate, the CPT resonance would split into a triplet. The splitting detuning refers to the modulation frequency. We explain it as following: the change of the light polarizations by electro-optic modulator, implying the relative phase variation between two linear polarizations, causes the phase modulation of the transition rabi frequencies, thus leading the CPT resonance splitting. This result also notices us the the laser polarization stability also plays a role in the CPT resonance especially while we purse the application of CPT with narrow linewidth, such as CPT clock.

References

1. M. Huang, J. C. Camaro, **PHYSICAL REVIEW A**, A85, 012509 (2012).
2. Peter Yun, Jean-Marie Danet, David Holleville, Emeric de Clercq, **APPLIIED PHYSICS LETTERS** 105, 231161 (2014).

B17

Effect of chloride ion in photoreaction of 4-aminobenzoic acid on silver surface investigated by the SERS spectroscopy and the DFT calculation

Do Geun Yoon, Hong Lae Kim, Chan Ho Kwon*
Department of Chemistry, Kangwon National University, Chuncheon 24341, Korea
**E-mail : chkwon@kangwon.ac.kr*

We study about photo-induced dimerization of 4-aminobenzoic acid (4ABA) on silver surface with hydrogen chloride. The aminobenzene derivatives, on silver surface, are easily going to its azo-compound when the laser irradiates. Also, it is well-known that the chloride anion is a competitive adsorbate on silver surface and it can change the orientation of the probe molecules. The SERS spectrum of 4ABA on silver surface is similar with one of the azobenzene-4,4'-dicarboxylic Acid. But the SERS spectrum of 4ABA on silver surface with the hydrogen chloride dose not changed, which is rather similar with the reported SERS spectrum of 4ABA. We analyzed the measured spectra comparing with the DFT calculations. We suggest that the chloride anion inhibits the photo induced dimerization of 4ABA through the competitive adsorption with NH_2 group and excess protons also inhibit it through the protonation of amino group.

References

1. J. S. Suh, D. P. DiLella, and M. Moskovits, *J. Phys. Chem.* 87, 1540-1544 (1983).
2. R. S. Venkatachalam, F. J. Boerio and P. G. Roth, *J. Raman Spectrosc.* 19, 281-287 (1988).
3. H. Park, S. B. Lee, K. Kim, and M. S. Kim, *J. Phys. Chem.*, 94, 7516-1580 (1990).

B18

Relative intensity of a crossover resonance to Lamb dips

Shoko Okuda and Hiroyuki Sasada
Department of Physics, Faculty of Science and technology, Keio University, 3-14-1, Hiyoshi,
Kohiku-ku, Yokohama 223-8522, Japan
JST, ERATO MINOSHIMA IOS Project, 1-5-1 Chofugaoka, Chofu, Tokyo 182-8585, Japan
e-mail: okudashoko@keio.jp

Crossover resonances (CORs) induced in three-level systems have been usually observed in saturated absorption spectroscopy of atoms and molecules together with a pair of Lamb dips. Recently, we observed CORs in Stark-modulation spectroscopy of the ν_3 band of methane [1]. Figure 1 shows observed spectra of the $P(4)\ E$, $Q(4)\ E$, and $R(4)\ E$ transitions with the selection rule of $\Delta M = \pm 1$. Each component of the triplets is assigned to two Lamb-dips from $|M''| = 2$ to $|M'| = 1$ and from $|M''| = 0$ to $|M'| = 1$, and the COR at the middle. The COR is the largest in intensity among the triplet in the Q- and R-branch transitions, while that is middle in the P-branch transition. To interpret the relative intensity of the CORs to the Lamb-dips, we use a set of rate equations for the three-level system and introduce two population decay rates for the upper and lower states. This simple model explains well the qualitative behavior of the relative intensity when the population decay rate of the upper state strongly depends on the Coriolis sublevels of the $v_3 = 1$ state.

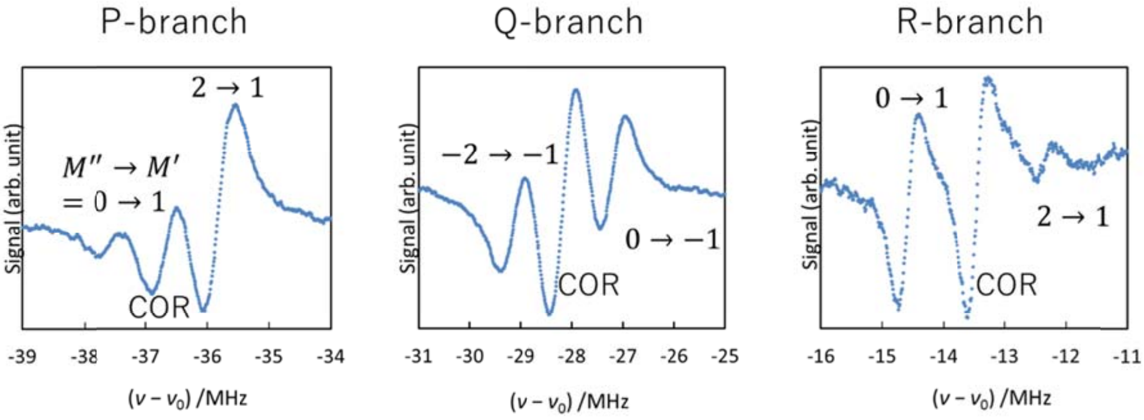

$P(4)\ E$, 22.5 kV/cm $Q(4)\ E$, 25.0 kV/cm $R(4)\ E$, 30.0 kV/cm

Figure 1. Observed triplets of COR and Lamb dips.

References

1. S. Okuda, H. Sasada, **J. Opt. Soc. Am. B**, *34*, 2558- (2017).

B19

The Influence of Atmospheric Helium on Secondary Time Standard

Ko Han Chen
Department of Physics, National Central University, Taiwan whykohan@gmail.com

For an optical frequency standard, there should be a reliable and time-independent reference like atomic transitions. Our group focused on observing the atomic spectrum of cesium 822nm two-photon transition. It is generally acknowledged that the energy gap of the atom is accurate so that it can determine an absolute frequency. We constructed a laser system, locked the laser frequency by electro-optical modulation and narrowed the laser linewidth by Pound-Drever-Hall technique to resolve an atomic spectrum. The results of the experiments indicated that the spectral positions were not exactly the same among ten commercial cesium cells [1]. However, the inconsistence of absolute frequencies among cells was perceived even all systematic errors had been considered, which the finding is serious in terms of building up a reliable optical reference for research. In 2014, N. D. Zameroski *et. al.* [2] indicated that helium gas might diffuse into the glass cell from the atmosphere, then shift atomic energy level and cause collision broadening. To prove the assumption, we observed two cells simultaneously. One was in the vacuum system and we prepared cesium atoms by heating a dispenser at 10^{-10} torr ultrahigh vacuum to ensure that the atom source was free from the collision of the residual gas. The other one was fixed in a chamber filled with 1.75 atm Helium for measuring the difference of linewidth and frequency shift. Compared with both of them, the difference of two spectra is highly related to the collision with Helium. Our experimental result showed that it would be suspicious to use glass cells as frequency references, especially for the long-term measurements like years.

References

1. C. M. Wu, T. W. Liu, M. H.Wu, R. K. Lee and W. Y. Cheng, ”Absolute frequency of Cesium 6S-8S 822 nm two-photon transition by a high-resolution scheme”, Opt. Lett. 38, 3186(2013)
2. N. D. Zameroski, G. D. Hager, C. J. Erickson, and J. H. Burke, “Pressure broadening and frequency shift of the 5S1/2 → 5D5/2 and 5S1/2 → 7S1/2 two photon transitions in 85Rb by the noble gases and N2”, J. Phys. B: At. Mol. Opt. Phys. 47 225205(2014)

B20

Dual-comb spectroscopy of acetylene ν_1+ν_3 vibration band

Kana Iwakuni[1,2,3*], **Sho Okubo**[2,3], **Koichi M. T. Yamada**[4], **Hajime Inaba**[2,3], **Feng-Lei Hong**[2,3,5]
and Hiroyuki Sasada[1,3]
[1]Keio University, [2]AIST/NMIJ, [3]JST, ERATO, [4]AIST/EMRI, [5]Yokohama National University,
*current affiliation; JILA, University of Colorado
e-mail: kana.iwakuni@jila.colorado.edu

An optical frequency comb (OFC), originally developed for frequency metrology, has drastically simplified frequency measurements in optical region. It also has provided new spectroscopic methods, in particular, dual-comb spectroscopy (DCS), in which two OFCs having slightly different repetition rates are used [1]. DCS enables us to measure broadband spectra with high resolution in a short time. And on the other hand the high frequency precision is maintained: the relative uncertainty in frequency is less than 10^{-13}. Using DCS, we recorded the ν_1 + ν_3 vibration band of acetylene ($^{12}C_2H_2$) with six different sample pressures and measured linewidth and line intensity. Figure 1 depicts pressure broadening coefficients for each ro-vibration transition determined from the analysis of the linewidth measurements. It indicates a clear zig-zag structure on the R-branch, even though it is less obvious on the P-branch due to the poor signal-to-noise ratio of the absorption lines. This ortho-para dependence of the pressure broadening coefficients has been observed for the first time, and we attributed it to the rotational resonance and the nuclear spin statistics [2]. We also analyzed the intensity of the dual-comb spectrum and determined the vibrational transition dipole moment [3], which was consistent in the magnitude with the previous work with FTIR within the discrepancy of 1%. These results have demonstrated that DCS opens new era of molecular spectroscopy.

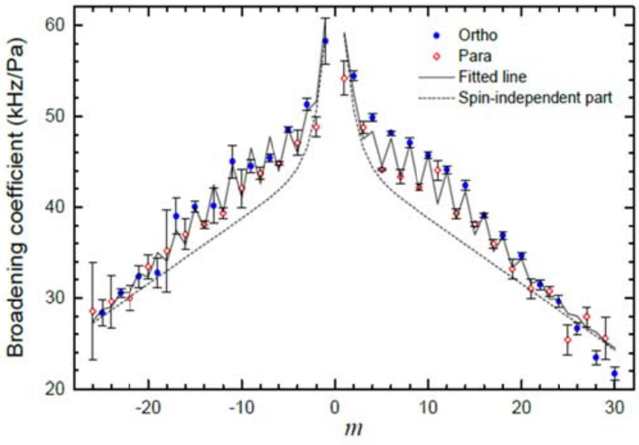

Figure 1. Pressure broadening coefficient for each

References

1. I. Coddington, N. Newbury, and W. Swann, **Optica**, 3, 414 (2016).
2. K. Iwakuni, S. Okubo, K M.T. Yamada, H. Inaba, A. Onae, F-L. Hong and H. Sasada, **Phys. Rev. Lett.** 117, 143902 (2016).
3. S. Okubo, K. Iwakuni, K. M. T. Yamada, H. Inaba, A. Onae, F-L. Hong, and H. Sasada, **J. Mol. Spectrosc.** 341, 10 (2017).

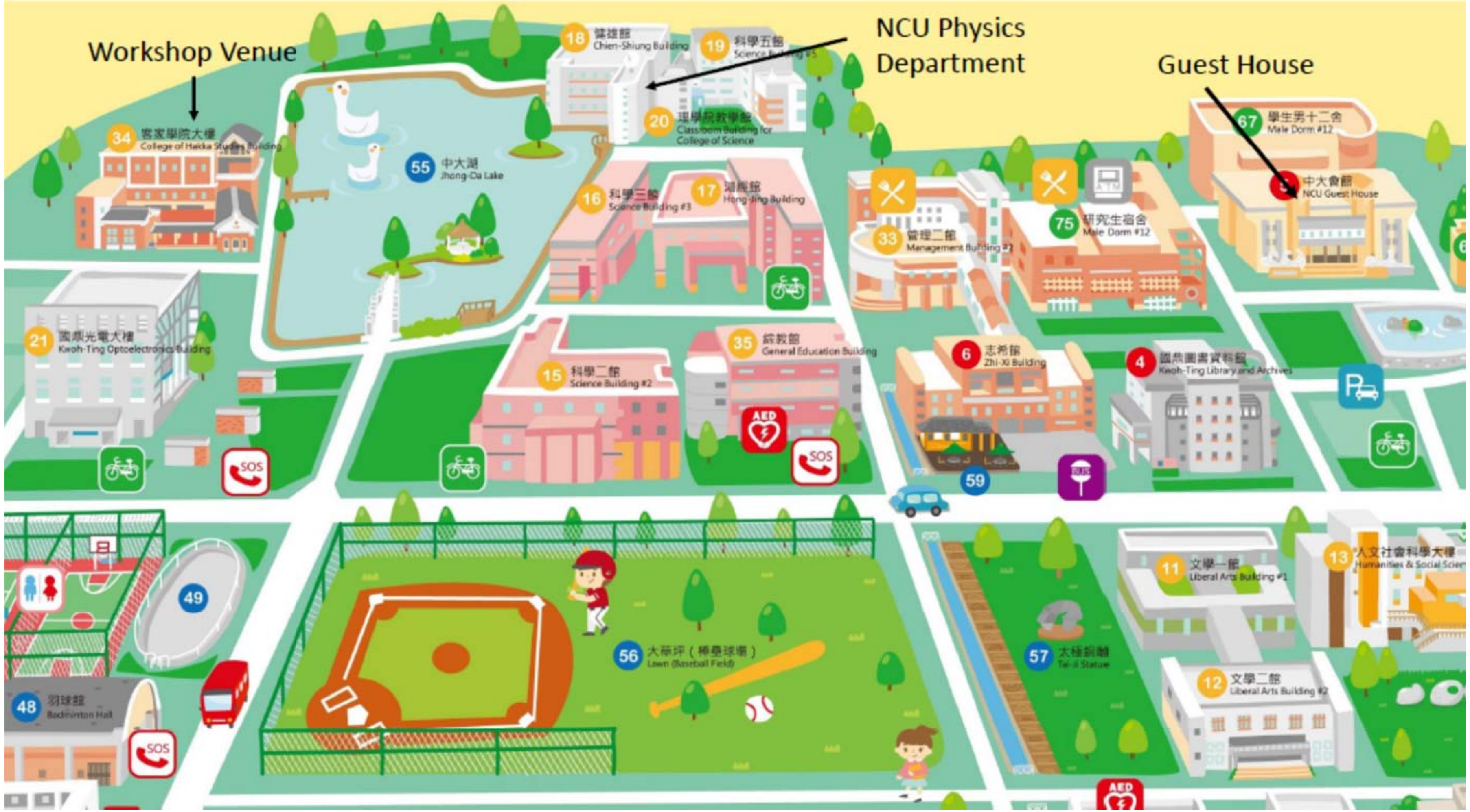
Workshop Venue
NCU Physics Department
Guest House
18 健雄館 Chien-Shiung Building
19 科學五館 Science Building #5
20 理學院教學館 Classroom Building for College of Science
34 客家學院大樓 College of Hakka Studies Building
55 中大湖 Jhong-Da Lake
16 科學三館 Science Building #3
17 鴻經館 Hong-Jing Building
33 管理二館 Management Building #2
75 研究生宿舍 Male Dorm #12
67 學生男十二舍 Male Dorm #12
中大會館 NCU Guest House
ATM
21 國鼎光電大樓 Kwoh-Ting Optoelectronics Building
15 科學二館 Science Building #2
35 綜教館 General Education Building
AED
SOS
6 志希館 Zhi-Xi Building
4 國鼎圖書資料館 Kwoh-Ting Library and Archives
59
BUS
49
48 羽球館 Badminton Hall
56 大草坪（棒壘球場） Lawn (Baseball Field)
57 太極銅雕 Tai-ji Statue
11 文學一館 Liberal Arts Building #1
12 文學二館 Liberal Arts Building #2
13 人文社會科學大樓 Humanities & Social Scien

Participants

First Name	Last Name	Affiliation	E-mail
Takayoshi	Amano	Jet Propulsion Laboratory, California Institute of Technology	tamano@jpl.nasa.gov
Kanaoka	Ayumi	Kyoto University	kanaoka.ayumi.55u@st.kyoto-u.ac.jp
Masaaki	Baba	Kyoto University	baba.masaaki.3n@kyoto-u.ac.jp
Malgorzata	Biczysko	Shanghai University	biczysko@i.shu.edu.cn
Carlos	Cabezas	National Chiao Tung University	ccabezas@nctu.edu.tw
Bor-Chen	Chang	National Central University	bchang@ncu.edu.tw
Yuan-Pin	Chang	National Sun Yat-sen University	ypchang@mail.nsysu.edu.tw
Lu-Chen	Chang	National Central University	jhanglujhen@icloud.com
Lu-Chen	Chang	National Central University	
Yu-Jung	Chen	National Central University	asperchen@phy.ncu.edu.tw
Jeng-En	Chen	National Central University	3z1415926z@gmail.com
Chiao-Wei	Chen	Academia Sinica	roger1208@gate.sinica.edu.tw
Guan-Hui	Chen	National Central University	ky86520@gmail.com
Shiang Ting	Chen	National Central University	shiang0609@gmail.com
Ko-Han	Chen	National Central University	
jeng-en	Chen	National Central University	
Ko-Hen	Chen	National Central University	paulxxxtw@gmail.com
Wei-Ling	Chen	National Tsing Hua University	chen821006@gmail.com
Wang-Yau	Cheng	National Central University	wycheng@ncu.edu.tw
Allan Shi Chung	Cheung	The University of Hong Kong	hrsccsc@hku.hk
Che-Yu	Chiang	National Sun Yat-sen University	silencecobra@hotmail.com
Myong Yyong	Choi	Gyeongsang National University	mychoi@gnu.ac.kr
Chi-Hsiang	Chu	National Central University	
Chuanxi	Duan	Central China Normal University	duanchx@mail.ccnu.edu.cn
Takayuki	Ebata	Hiroshima University	tebata@hiroshima-u.ac.jp
Yasuki	Endo	National Chiao Tung University	endo@nctu.edu.tw
Katsunari	Enomoto	University of Toyama	enomoto@sci.u-toyama.ac.jp
Gang	Feng	Chongqing University	fengg@cqu.edu.cn
Masaru	Fukushima	Hiroshima City University	fukushim@info.hiroshima-cu.ac.jp
Qian	Gou	Chongqing University	qian.gou@cqu.edu.cn
Karolina	Haupa	National Chiao Tung University	karolina.haupa@gmail.com
Shih-Hsiang	Hong	National Central University	eric455489@gmail.com
Jon	Hougen	NIST	jon.hougen@nist.gov

Yen-Chu	Hsu	National Central U.	ychsu@po.iams.sinica.edu.tw
Tsai-Lin	Hsu	National Central University	lithium0915@gmail.com
Xixi	Hu	Nanjing University	xxhu@nju.edu.cn
Qian-Rui	Huang	Academia Sinica	append@gmail.com
Jing	Huang	Nanjing University	huangj@smail.nju.edu.cn
Kana	Iwakuni	JILA	kana.iwakuni@jila.colorado.edu
Ye-Jin	Kim	Ulsan National Institute of Science and Technology	gne1019@unist.ac.kr
Kaori	Kobayashi	University of Toyama	kaori@sci.u-toyama.ac.jp
Jer-Lai	Kuo	IAMS, Academia Sinica	jlkuo@pub.iams.sinica.edu.tw
Oh-Hoon	Kwon	Ulsan National Institute of Science and Technology	ohkwon@unist.ac.kr
Yuan-Pern	Lee	National Chiao Tung University	yplee@mail.nctu.edu.tw
Sang	Lee	Pusan National University	sklee@pusan.ac.kr
Hui	Li	Jilin University	Prof_huili@jlu.edu.cn
wei che	Liang	National Chiao Tung University	j821005@gmail.com
Hsin-Yi	Liao	National Taipei University of Education	hyliao@tea.ntue.edu.tw
King-Chuen	Lin	National Taiwan Univ.	kclin@ntu.edu.tw
Tze-Wei	Liu	National Central University	b91202001@gmail.com
Jing-Min	Liu	Jilin University	liujm14@mails.jlu.edu.cn
Pei-Ling	Luo	National Chiao Tung University	kkmion@gmail.com
Anthony	Merer	University of British Columbia	merer@chem.ubc.ca
Masatoshi	Misono	Fukuoka University	m-misono@fukuoka-u.ac.jp
Kenta	Mizuse	Tokyo Institute of Technology	mizuse@chem.titech.ac.jp
Kyeong-Eun	Mun	Ulsan National Institute of Science and Technology	mke3321@unist.ac.kr
Hak-won	Nho	Ulsan National Institute Science and Technology	icize13@unist.ac.kr
De-Chen	Nien	National Central University	
Shoko	OKUDA	Keio university	okudashoko@keio.jp
Won-Woo	Park	Ulsan National institute of Science and Technology	b0603@unist.ac.kr
Jae-Heon	Park	Ulsan National Institute of Science and Technology	jhpark5107@unist.ac.kr
Wei	Ren	The Chinese University of Hong Kong	renwei@mae.cuhk.edu.hk
Hiroyuki	Sasada	Keio University	sasada@phys.keio.ac.jp
Thomas	Schultz	Ulsan National Institute of Science and	schultz@unist.ac.kr

		Technology (UNIST), Korea	
Yu-Jhe	Shih	National Central University	
Pavithraa	Sundararajan	National Chiao Tung University	pavi.nctu@gmail.com
Ying-Chin	Sung	National Central University	jing821005@gmail.com
Kaito	Takahashi	IAMS, Academia Sinica	kt@gate.sinica.edu.tw
Keiichi	Tanaka	Kyushu University	ktanaka@chem.kyushu-univ.jp
Dianmin	Tong	Shandong University	tdm@sdu.edu.cn
Yung-Hsu	Tseng	Academia Sinica	flyswimcamel@hotmail.com
Masashi	Tsuge	Hokkaido University	tsuge@lowtem.hokudai.ac.jp
Wen-Bih	Tzeng	IAMS, Academia Sinica	wbt@sinica.edu.tw
Yi Jen	Wang	IAMS, Academia Sinica	edith043@gmail.com
Yin	Wang	Healthy Photon Co., Ltd.	yin.wang@healthyphoton.com
Kyohei	Watanabe	University of Toyama	d1671205@ems.u-toyama.ac.jp
Yu-Jong	Wu	NSRRC	yjwu@nsrrc.org.tw
Li-Hong	Xu	University of New Brunswick	lxu@unb.ca
Hsin-Fu	Yang	National Central University	yang869650@gmail.com
Yukiko	Yarnall	George Mason University	yyarnall@masonlive.gmu.edu
Cangtao	Yin	IAMS, Academia Sinica	ctyin1986@gmail.com
Do Geun	Yoon	Kangwon National University	puri102@nate.com
Hsin-Hung	Yu	National Central University	
Yu	Zhai	Jilin University	yuzhai@mail.huiligroup.org